DELPHI Collaboration

DELPHI 2001-027 CONF 468
14 March, 2001

Determination of A_{FB}^{b} using inclusive charge reconstruction and lifetime tagging at LEP 1

K.Münich[1], M.Elsing[2], B.Schwering[1], T.Allmendinger[3], G.Barker[3], M.Feindt[3], C.Haag[3]

Abstract

A novel method is used to measure the b quark forward-backward asymmetry at the Z pole on a sample of 2,636,000 hadronic events collected with the DELPHI detector in 1992 to 1995. An enhanced impact parameter tag is applied to the data to obtain a high purity b sample. For each event hemisphere the charge of the corresponding quark or anti-quark is determined using a neural network tag which combines in an optimal way the full available charge information from the vertex charge, the jet charge and from identified leptons and hadrons. The probability to correctly identify b quarks and anti-quarks is calibrated on data itself comparing the rates of double hemisphere tagged like-sign and unlike-sign events. The b quark forward-backward asymmetry is determined from the differential asymmetry taking small corrections due to hemisphere correlations and background contributions into account. The result is:

$$A_{FB}^{\mathrm{b}}\ (91.26\ \mathrm{GeV}) \quad = \quad 0.0931 \pm 0.0034(\mathrm{stat.}) \pm 0.0017(\mathrm{syst.})$$

The effective weak mixing angle is deduced from the measurement to be:

$$\sin^2\theta_{\mathrm{eff}}^{\ell} \quad = \quad 0.23287 \pm 0.00068$$

Preliminary results for the 2001 Moriond Conference

[1] Fachbereich Physik, University of Wuppertal, Postfach 100127, D-42097 Wuppertal, Germany
[2]CERN, CH-1211 Geneva 23, Switzerland
[3] Institut für Experimentelle Kernphysik, Universität Karlsruhe, Postfach 6980, D-76128 Karlsruhe, Germany

1 Introduction

The measurements of the b quark forward-backward asymmetry at the Z pole provide the most precise determination of $\sin^2\theta^{\ell}_{\rm eff}$ at LEP. For pure Z exchange and to lowest order the forward-backward pole asymmetry of b quarks, $A^{0,\rm b}_{FB}$, can be written in terms of the vector and axial-vector couplings of the initial electrons $(v_{\rm e}, a_{\rm e})$ and the final b quarks $(v_{\rm b}, a_{\rm b})$:

$$A^{0,\rm b}_{FB} = \frac{3}{4}\frac{2a_{\rm e}v_{\rm e}}{a^2_{\rm e}+v^2_{\rm e}}\frac{2a_{\rm b}v_{\rm b}}{a^2_{\rm b}+v^2_{\rm b}} \tag{1}$$

Higher order electroweak corrections are taken into accounted by means of an improved Born approximation [1], which leaves the above relation unchanged, but defines the modified couplings ($\bar{a}_{\rm f}$, $\bar{v}_{\rm f}$) and an effective mixing angle $\theta^{\rm f}_{eff}$:

$$\frac{\bar{v}_{\rm f}}{\bar{a}_{\rm f}} = 1 - 4|q_{\rm f}|\sin^2\theta^{\rm f}_{eff} \tag{2}$$

$q_{\rm f}$ is the electric charge of the fermion. The b quark forward-backward asymmetry determines the ratio of these couplings. Therefore it is basically sensitive to the $\sin^2\theta^{\ell}_{\rm eff}$ defined by the ratio of the electron couplings.

The current LEP average of $\sin^2\theta^{\ell}_{\rm eff}$ (see [2]) deviates by about 2.5 standard deviations from the corresponding SLD result determined from the left-right cross section asymmetry, A_{LR}. Hence additional and more precise $A^{0,\rm b}_{FB}$ measurements are of special interest. In this paper a measurement of $A^{0,\rm b}_{FB}$ is presented based on a very powerful new b quark charge tagging technique.

Previously established methods to measure the b quark forward-backward asymmetry in DELPHI [4, 5] were either exploiting the charge correlation of the semileptonic decay lepton (muon or electron) to the initial b charge or were using the jet charge information in selected b events. These methods suffer from the limited charge tagging efficiency, because of the relatively small semileptonic branching ratio or because of the small jet charge separation between a b quark and anti-quark jet.

This analysis improves on the charge tagging efficiency by using the full available experimental charge information from b jets. The excellent DELPHI micro vertex detector separates the particles from b hadron decays from fragmentation products on the basis of the impact parameter measurement. The hadron identification capability provided by the DELPHI Ring Imaging Cherenkov Counters provide a means of exploiting charge correlations of kaons or baryons in b jets. This allows not only to measure directly the secondary b decay vertex charge, but also to obtain further information for a single jet, like the decay flavour for the different b hadron types ($\rm B^0$, $\rm B^+$, $\rm B_s$ and b-baryon). A set of Neural Networks is used to combine the additional input with the lepton and jet charge information in an optimal way.

In order to fully exploit the much improved b charge tagging a new self-calibrated method to extract the forward-backward asymmetry was developed. The b quark charge is reconstructed in both event hemispheres for a high purity sample of b events, selected using an enhanced impact parameter tag. Comparing the rate of double hemisphere tagged like-sign and unlike-sign events it is possible to extract the charge tagging efficiency directly from the data. The b quark forward backward asymmetry is determined from the differential asymmetry of the two samples of single tagged and unlike-sign double

tagged events. Here small corrections due to residual background contributions and due to charge tagging hemisphere correlations are taken into account.

The paper is organised as follows. First a short summary of the hadronic event selection is given. In section 3 the b event tagging used to obtain the high purity b quark sample is described. Section 4 details the charge tagging technique using Neural Networks and the self-calibrating method to extract the forward backward asymmetry. Section 5 describes the measurement of A_{FB}^{b} on the DELPHI data of 1992 to 1995. Section 6 discusses the systematic errors. Finally the conclusion is given in section 7. Technical information on the self-calibration method can be found in the appendix at the end of the paper.

2 Selection of Z decays to hadrons

A detailed description of the DELPHI apparatus [†] can be found in [6] and in the references therein. This analysis makes full use of the information provided by the tracking system, the calorimetry and the detectors for hadron and lepton identification. Of special importance is the silicon vertex detector providing three precise $R\phi$ measurements. For 1994 and 1995 the extended detector accepted particles down to low θ (25°) and provided z measurements in the closest and outer shells.

This paper uses DELPHI data taken at LEP 1 from 1992 to 1995 at centre-of-mass energies in an interval of ± 0.5 GeV around the Z pole. For events entering the analysis nominal working conditions during data taking are required at least for the central tracking detector TPC and for the electromagnetic calorimeters and the muon detector system. The operating conditions and efficiency of the RICH detectors varied strongly for the different data sets. These variations are included in the corresponding simulated data samples.

charged particle momentum	$\geq$	0.4 GeV/c
neutral particle energy	$\geq$	1.0 GeV
track length (tracks measured only with TPC)	$\geq$	30 cm
polar angle	$\geq$	20°
uncertainty of the momentum measured	$\leq$	100 %
impact parameter ($R\phi$)	$\leq$	4 cm
impact parameter (z)	$\leq$	10 cm

Table 1: *Cuts to select well measured tracks.*

For each event cuts are applied to the measured particles to ensure both good quality of the reconstruction and also good agreement of data and simulation. The selections are summarised in Table 1. In addition for neutral clusters measured in the calorimeters the reconstructed shower energy had to below 50 GeV for the HPC and HAC, 30 GeV for the EMF and 20 GeV for the STIC/SAT.

[†] In the DELPHI coordinate system the z-axis is the direction of the e^- beam. The radius R and the azimuth angle ϕ are defined in the plane perpendicular to z. The polar angle θ is measured with respect to the z-axis.

total energy of charged particles	$\geq$	$0.15 \times \sqrt{s}$
sum of the energy of charged particles in a hemisphere	$\geq$	$0.03 \times \sqrt{s}$
total multiplicity of charged particles	$\geq$	7
multiplicity of charged particles in hemisphere	$\geq$	1
$\cos(\theta_{\vec{T}})$	$\in$	$[-0.9, +0.9]$

Table 2: *Selections for Z decays to hadrons. $\sqrt{s}$ is the centre-of-mass energy.*

A second step selects Z decays to hadrons as in Table 2. Here each event is divided into two hemispheres by the plane perpendicular to the thrust axis, $\vec{T}$, which is computed using the charged and neutral particles. $\theta_{\vec{T}}$ is the polar angle of the thrust axis. In addition the negligible number of events are discarded which contain at least one reconstructed particle with an unphysically high momentum above 500 GeV/c.

year	data	simulation	$\langle\sqrt{s}\rangle$
1992	600856	1576841	91.280 GeV
1993	424781	1686345	91.225 GeV
1994	1226265	2851888	91.202 GeV
1995	384099	1084865	91.288 GeV

Table 3: *Number of selected Z decays to hadrons for the different years of data taking.*

These select $2.636 \cdot 10^6$ Z decays to hadrons at a mean centre-of-mass energy of 91.234 GeV (see Table 3). The remaining backgrounds due to τ, Bhabha, and $\gamma\gamma$ events as well as contributions from beam-gas or beam-wall interactions are small and are safely neglected in the following.

The data is compared to $7.2 \cdot 10^6$ fully simulated hadronic decays using JETSET 7.3 [7] with DELPHI tuning of fragmentation, b production and decay parameters [8].

3 Selection of Z decays to b quarks using an enhanced impact parameter method

Decays to b quarks are selected from the sample of hadronic Z decays using the DELPHI high purity b tagging. The technique is based on the well established impact parameter method [9], adopted by DELPHI for the precision measurement of R_b [10, 11]. The analysis uses the apparent lifetime and the invariant mass of the reconstructed secondary decay as well as the transverse momentum and rapidity of charged particles and identified leptons with respect to the jet direction as reconstructed with the LUCLUS algorithm [7].

In this analysis uses a combined event tagging probability variable, b_{tag}. Decays to b quarks tend to have higher b_{tag} values whereas decays to other quarks are peaked at smaller values as can be seen in Figure 1. High purity samples are selected by cutting on b_{tag}.

It is important to avoid a bias in the background estimates due to an imperfect description of the tagging performance in the simulation. Therefore the purities of b , c and

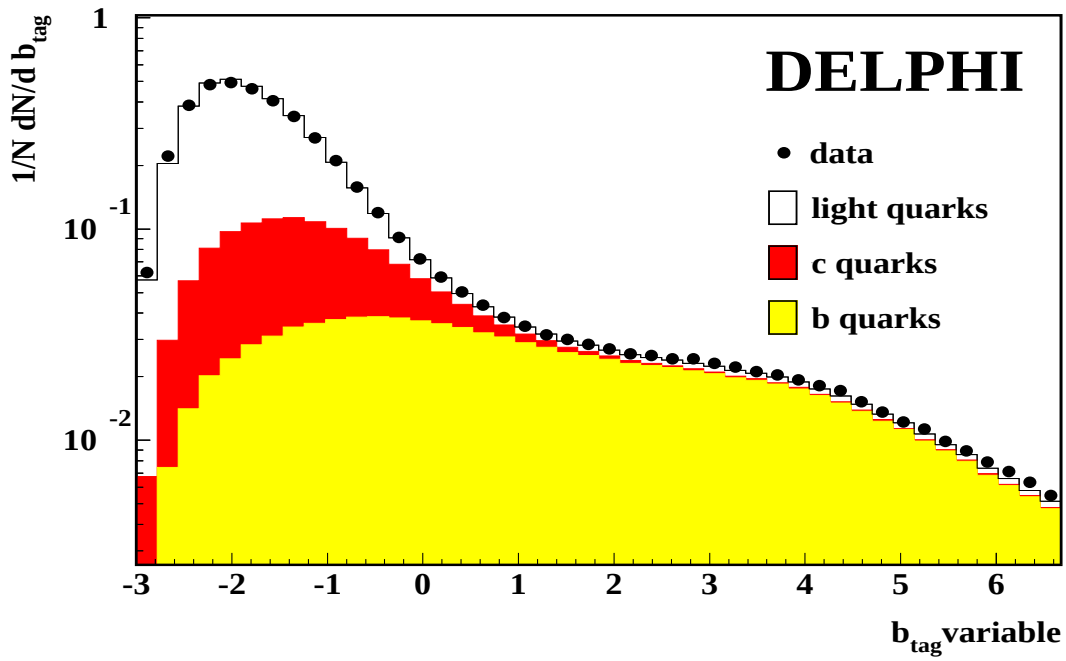

Figure 1: *Comparison between data and simulation of the normalised number of events versus the* b_{tag} *variable (for 1994 data). Light quark,* c *quark, and* b *quark events are shown separately for the simulation.*

light flavours and the efficiency for b quark events, ϵ_b, are measured directly from the data. ϵ_b is measured from the data using:

$$\epsilon_b(cut) = \frac{\mathcal{F}(cut) - R_c \times \epsilon_c(cut) - (1 - R_c - R_b) \times \epsilon_{uds}(cut)}{R_b} , \tag{3}$$

where $\mathcal{F}$ is the fraction of selected events at a given cut value. ϵ_{uds} and ϵ_c are the selection efficiencies for the light flavours and the charm events, which are both obtained from the simulation. The fractions of c and b events produced in hadronic Z^0 decays, R_c and R_b, are set to the LEP average values of $R_c = 0.1709 \pm 0.0034$ and $R_b = 0.21653 \pm 0.00069$ [3]. The corresponding purities, p_f, are then calculated for each flavour using:

$$p_f(cut) = \epsilon_f(cut) \times \frac{R_f}{\mathcal{F}(cut)} . \tag{4}$$

Accurate tuning of the simulation to the data was performed [10, 11] in order to estimate the c and light flavour background efficiencies correctly. Here each year of data taking is treated separately to allow for the changes in the detector performance. The simulated data has also been reweighted in order to represent the measured composition and lifetimes of charmed hadrons (see Table 7) and also the rate of gluon splitting into $c\bar{c}$ ($b\bar{b}$) pairs correctly.

The applied cuts of b_{tag} and the corresponding b purities and efficiencies for data and simulation are shown in Table 4. The simulation underestimates the performance of the b tagging compared to data. The same behaviour was already observed in reference [11] using a double tagging technique to calibrate the b efficiency on data to measure R_b. A working point at a very high b purity of $\sim$ 93 % is chosen to minimise systematic

year	cut on b_{tag}	p_b [%]		ϵ_b [%]	
		data	sim.	data	sim.
1992	-0.1	93.5	93.2	56.3	53.6
1993	-0.1	93.3	93.0	57.6	54.8
1994	0.1	92.5	92.1	67.2	63.7
1995	0.1	92.8	92.4	66.9	62.9

Table 4: *Summary of* b_{tag} *cuts and the resulting purity,* p_b*, and efficiency,* ϵ_b*, for data and simulation.*

uncertainties due to background estimations. The remaining background is dominated by about 70 % from decays to c quarks, which is taken into account in the systematic error study.

4 The inclusive charge tagging

This section explains the novel method for inclusive b charge tagging. First the experimental information and the neural network technique used to extract the b quark flavour information from the DELPHI data is described. In the second part the self-calibrating method to extract the b quark forward-backward asymmetry is explained. This includes the technique to determine the tagging probability on data as well as a discussion of the hemisphere charge correlations and background corrections.

4.1 The Neural Network method for inclusive Charge Tagging

The analysis uses the full available experimental charge information from b jets which is combined into one tagging variable using a Neural Network technique. The tagging method is part of a DELPHI common analysis package for b physics called BSAURUS [13]. In this paper only an overview of the package is given. For full details refer to reference [13].

The quark flavour tagging Neural Network is designed to distinguish between hemispheres originating from a b quark or anti-quark in $Z \longrightarrow b\bar{b}$ decays. The approach used is to construct a conditional probability for a given track to have the same charge as the b quark in the b hadron for both, the moment of fragmentation (i.e. production) and at the moment of decay. In addition, the probabilities are constructed separately for each of the b hadron types (B^+, B^0, B_s and b baryon). These probabilities are then combined with the jet charge and vertex charge information [‡] in the final Neural Network.

The first step to achieve this goal is to train a Neural Network with target output values of +1 and -1 if the charge of a particle is correlated or anti-correlated to the b quark charge. A set of predefined input variables is used to distinguish between them:

- **Selection variable for particles from secondary vertices:** The Neural Network called Tk_{net} separates particles originating from the event primary vertex from those starting at a secondary decay vertex. The separation uses the impact parameter measurement and additional kinematic information. Particles from the primary

[‡]For definitions see Equations 8 and 9 below.

vertex lead to Tk_{net} values close to 0, while particles from a secondary vertex get values close to 1.

- **Particle identification variables:** Lepton and hadron identification information is combined into tagging variables for kaons, protons, electrons, and muons from heavy hadron decays.

- $B - D$ **separation:** A dedicated Neural Network called BD_{net} uses decay vertex and kinematic information in a given jet to separate particles from the weak B decay from those from the subsequent cascade D decay. The target values for for particles from B decay is -1, while for particles from D decay it is +1. A second variable:

$$\frac{BD_{net} - BD_{net}^{min}}{\Delta BD_{net}} \tag{5}$$

  is constructed to further isolate particles from D decays. Here again the BD_{net} is the $B - D$ Neural Network introduced above. BD_{net}^{min} is the minimum BD_{net} value of all charged particles in the hemisphere above a BSAURUS Tk_{net} value of 0.5. ΔBD_{net} is the difference between the maximum and minimum value of BD_{net} for all charges particles.

- **Particle variables:** Further variables of carged particles separate particles from the primary iteraction from B decays. The energy of the particle and the BSAURUS "internal track quality flag" are input to the Networks. In addition particles are boosted into the estimated B candidate rest frame. In this frame the momentum and the helicity angle of the particle with respect to the B direction of flight are calculated.

- **Hemisphere variables:** For each hemisphere a set of additional variables characterise the quality of the B candidate:

  - the ratio of the reconstructed B candidate energy to the LEP beam energy,
  - the reconstructed secondary vertex mass,
  - the χ^2 probability of the secondary vertex fit,
  - the error on the vertex charge measurement,
  - the number of charged particles assigned to secondary vertices in the hemisphere passing a cut of $Tk_{net} > 0.5$,
  - the hemisphere rapidity gap between the particles of highest rapidity below a Tk_{net} cut at 0.5 and that of smallest rapidity above the cut at 0.5 and
  - the BSAURUS internal hemisphere quality flag.

The networks using charged particles to distinguish the decay flavour use all input variables described above. The lepton identification and B-D separation variables do not depend on the fragmentation flavour and are therefore not used in the training of the fragmentation flavour networks.

The particle correlation conditional probabilities, $P^{time}(same\, Q_B)$, for the fragmentation and the decay flavour are then combined using a likelihood ratio to obtain a flavour tag for a given hemisphere:

$$F_B^{time} = \sum_{particles} \ln\left(\frac{1+P^{time}(same\, Q_B)}{1-P^{time}(same\, Q_B)}\right)\cdot Q\ . \tag{6}$$

$B = B^+, B^0, B_s$ or b baryon and *time* stands for *fragmentation* or *decay*. Q is the particle charge. Depending on the hypothesis considered a different selection is applied for particles entering the summation. For the fragmentation flavour all tracks with $Tk_{net} < 0.5$ are considered, while for the decay flavour a particle must satisfy $Tk_{net} \geq 0.5$. The output of the hemisphere tags are shown in Figure 2 for the different fragmentation and decay tags.

Based on the hemisphere flavour tags defined above the final flavour tagging Neural Network is constructed. The first set of inputs is a combination of these fragmentation and decay flavour tags multiplied by the individual probabilities for that b hadron type:

(1) $F_{B_s}^{Frag.}\cdot P(B_s)$

(2) $\left(F_{B^+}^{Dec.} - F_{B^+}^{Frag.}\right)\cdot P(B^+)$

(3) $\left(F_{baryon}^{Dec.} - F_{baryon}^{Frag.}\right)\cdot P(baryon)$

(4) $\left(F_{B^0}^{Dec.}\cdot\left(1-2\sin^2(0.237\cdot\tau)\right) - F_{B^0}^{Frag.}\right)\cdot P(B^0)$

Here τ is the reconstructed B lifetime. The construction takes account of the B^0 oscillation frequency which affects the charge information in the hemisphere. This is not possible for the case of B_s where the oscillations are so fast that we have essentially a 50-50 mix of B_s and $\bar{B}_s$.

The $P(B)$ factors are the outputs of dedicated BSAURUS B species identification Network which represent probabilities that the hemisphere in question contains a weakly decaying hadron of a particular type B. These probabilities are shown in Figure 3. The input variables 1-4 are shown in Figure 4.

The remaining inputs are:

(5-7) The so called jet charge defined as:

$$Q_J = \frac{\sum_{particles}|p_L|^\kappa\cdot Q}{\sum_{particles}|p_L|^\kappa}, \tag{7}$$

where the sum is over all particles and p_L is the longitudinal momentum component w.r.t. the thrust axis. The optimal choice of the free parameter κ depends on the type of b hadron under consideration. Therefore a range of values ($\kappa = 0.3, 0.6, \infty$) are used, where the last one corresponds to taking the charge of the stiffest track in the hemisphere.

(8) Vertex charge is constructed using the Tk_{net} value as a probability for each track to originate from the b hadron decay vertex. A weighted vertex charge is formed by:

$$Q_v = \sum_{particles} Tk_{net}\cdot Q\ . \tag{8}$$

(9) The significance of the vertex charge calculated using a binomial error estimator:

$$\sigma(Q_v) = \sum_{particles} \sqrt{Tk_{net} \cdot (1 - Tk_{net})} \; . \tag{9}$$

Distributions of these input variables in data and simulation are shown in Figure 5.

In addition to the flavour discriminating variables described above, use is made of 'quality' variables, e.g. the reconstructed energy of B candidate in the hemisphere. These inputs supply the network during the training process with information regarding the likely quality of the discriminating variables, and are implemented in the form of weights to the turn-on gradient (or 'temperature') of the sigmoid function used as the network node transfer function. This construction guarantees a network output that is implicitly symmetric with respect to particle charge, which is clearly an important requirement for this analysis.

The training of the networks uses a standard feed-forward algorithm. The final Network utilises an architecture of 9 input nodes, one for each of the variables defined above, a hidden layer containing 10 nodes and one output node. During the training, the target values at the output node for one hemisphere were -1 or 1 for a b quark for an anti-quark.

An example of the flavour tag Neural Net output, $flav_{\rm hem}$, on the selected high purity b event sample is shown in Figure 6 for the data of 1994. The data points are compared to the simulation. The contributions from hemispheres containing b quarks and anti-quarks are shown separately for the simulation to illustrate the excellent charge separation. The difference between data and simulation in the width of the distribution indicates a small difference in the charge tagging efficiency which will be discussed in detail in the following.

In the analysis a hemisphere is flavour tagged, if the experimental information is sufficient to produce a Neural Network output $|flav_{\rm hem}|$ which exceeds the work point cut value of 0.35.

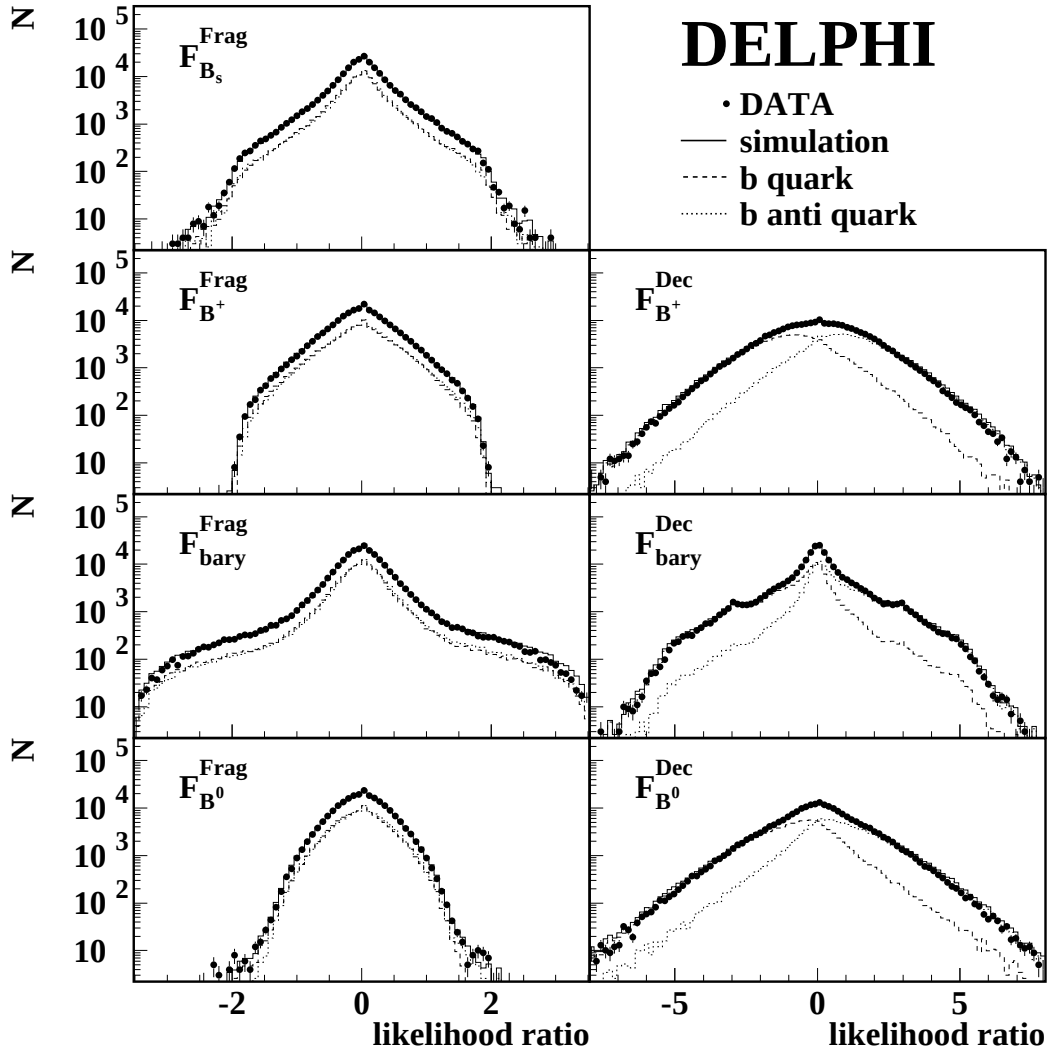

Figure 2: *The flavour hemisphere tag for the time of the fragmentation for the B^+, B^0, B_s and b baryon hypothesis and for the time of the decay for B^+, B^0 and b baryon hypothesis. Shown is the comparison between data and simulation for the data of 1994.*

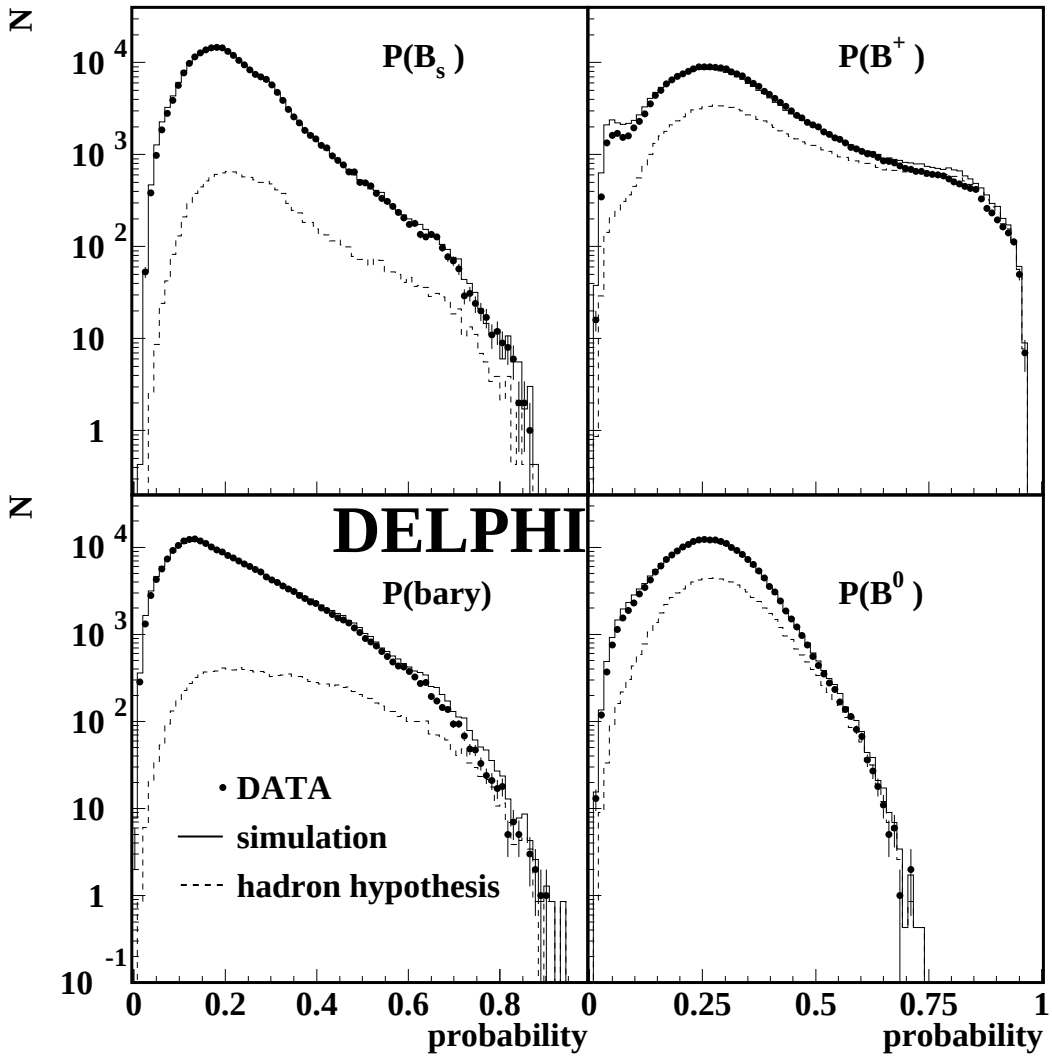

Figure 3: *The hemisphere constructed probabilities for the different b hadron types B^+, B^0, B_s and b baryon. Shown is the comparison between data and simulation for the data of 1994.*

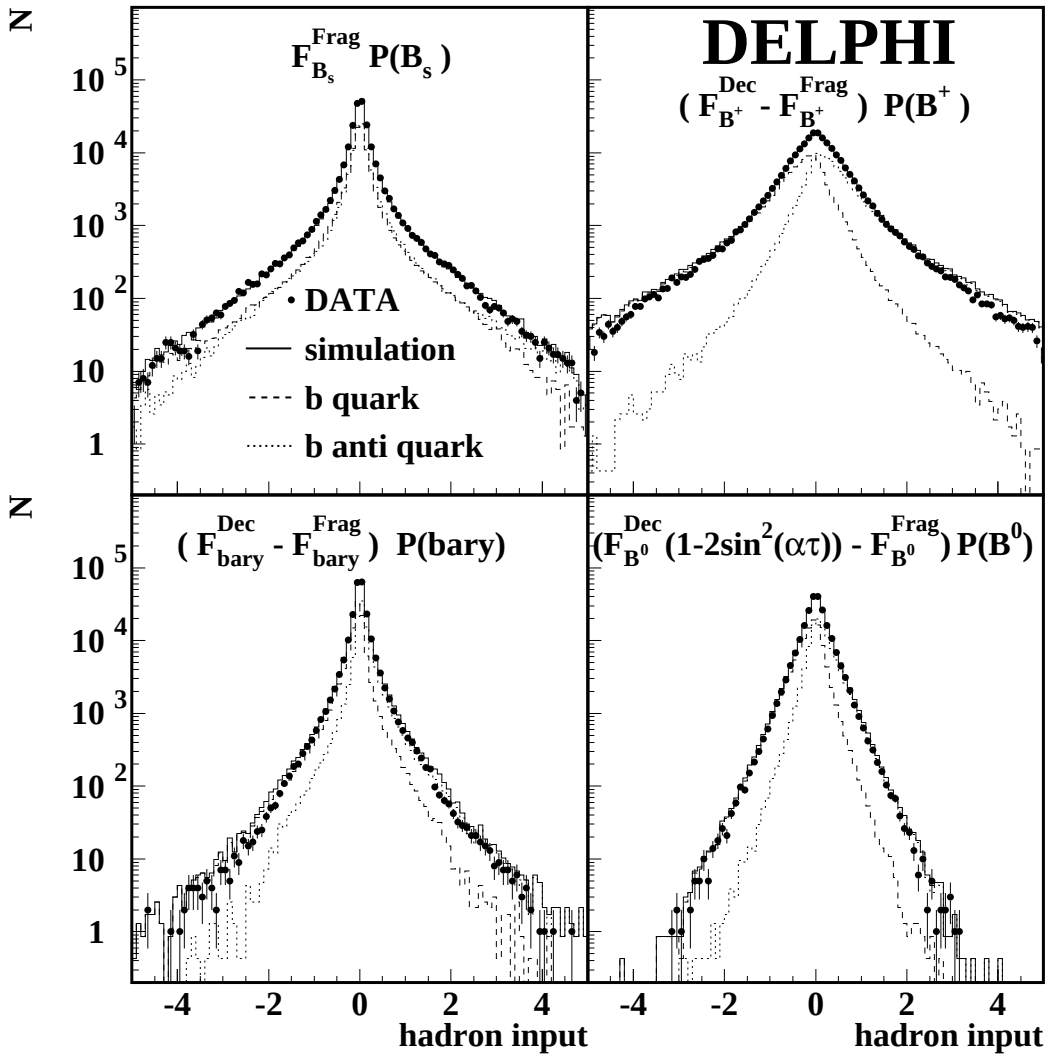

Figure 4: *The four combined hemisphere charge probabilities for the B^+, B^0, B_s and b baryon hypothesis. Shown is the comparison between data and simulation for the data of 1994.*

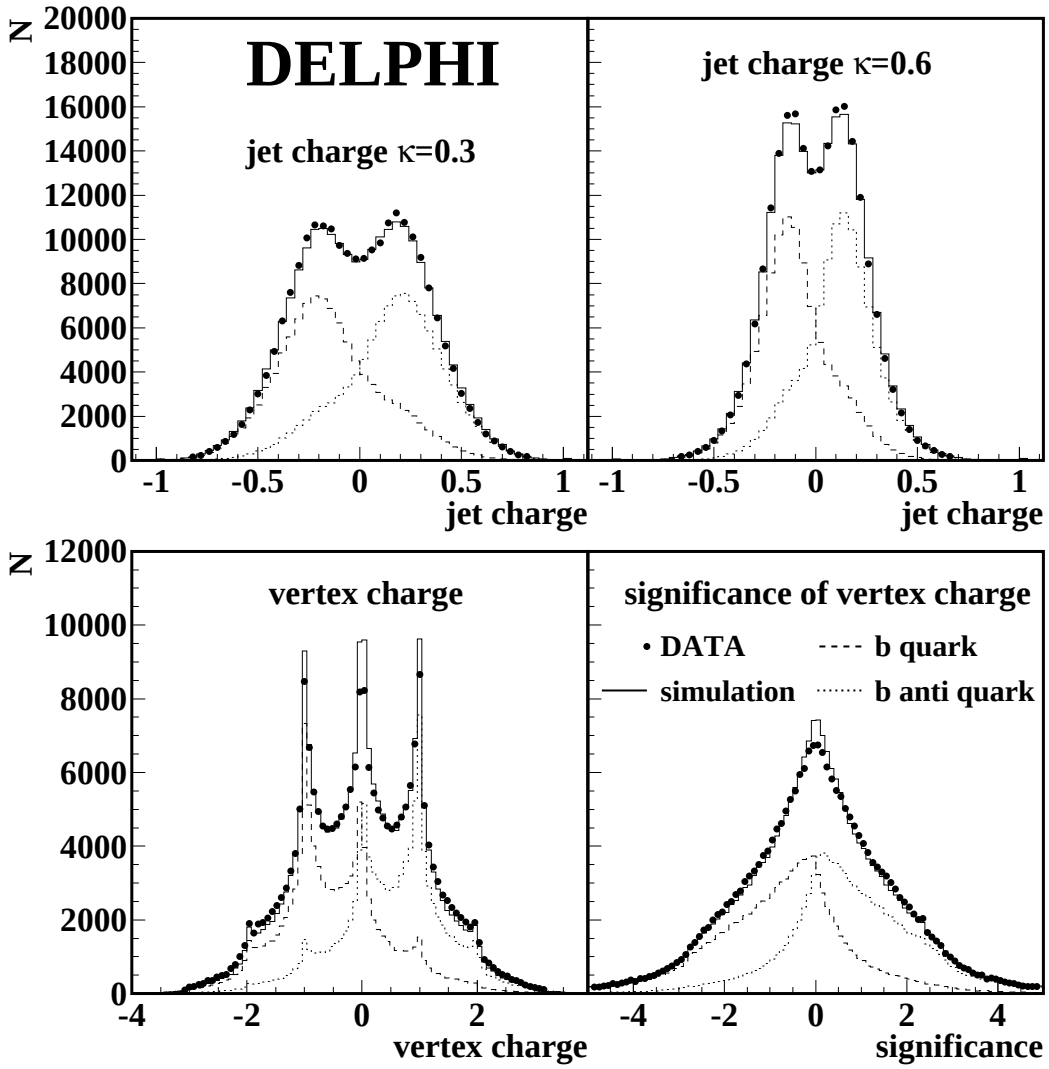

Figure 5: *The jet charge information for* $\kappa = 0.3$ *and* 0.6 *(upper plots) and the vertex charge and its significance (lower plots). Shown is the comparison between data and simulation for the data of 1994.*

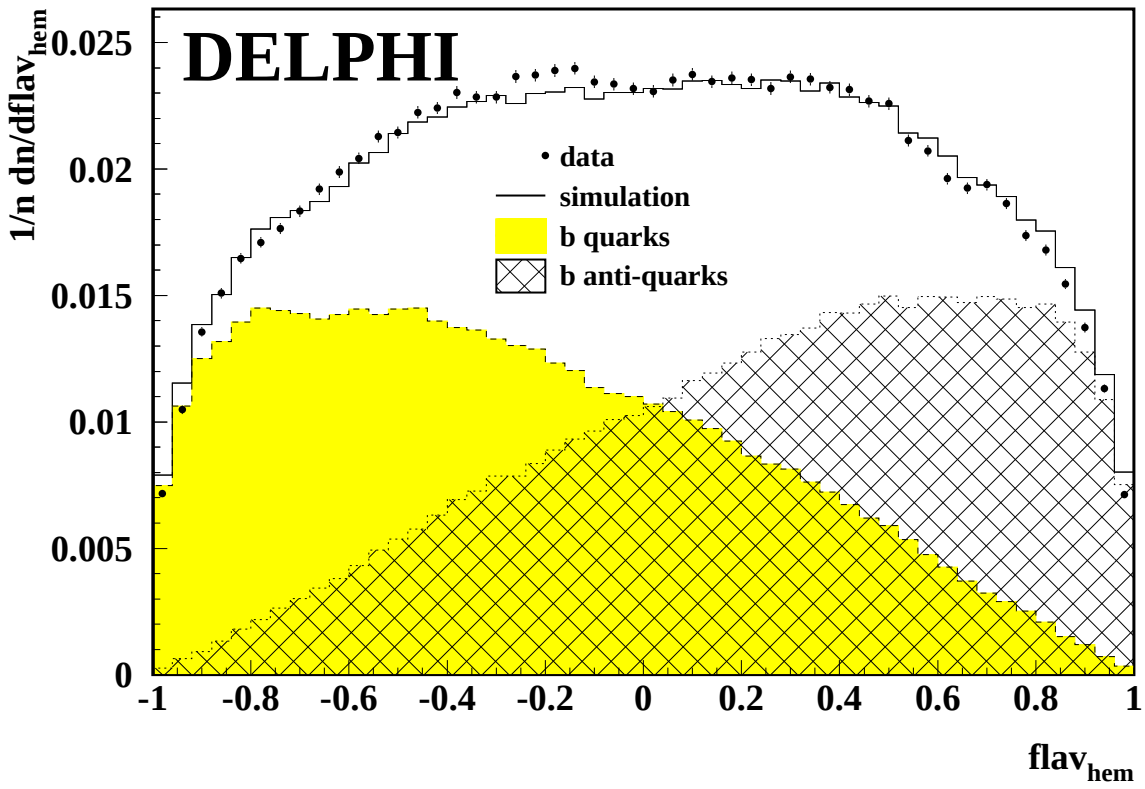

Figure 6: *Comparison between data and simulation for the flavour tag Neural Network output, $flav_{hem}$, for the data of 1994.*

4.2 Principles of the method to extract the b asymmetry

The differential cross section for b quarks from the process $e^+e^- \to Z \to b\bar{b}$ as a function of the polar angle θ can be expressed as :

$$\frac{d\sigma}{d\cos\theta} \propto 1 + \frac{8}{3} A_{FB}^{\mathrm{b}} \cos\theta + \cos^2\theta \,. \tag{10}$$

Hence the forward-backward asymmetry generates a $\cos\theta$ dependent asymmetry in the production of b quarks. For anti-quarks the orientation (sign) of the production polar angle is reversed.

In the analysis the thrust axis is used to approximate the quark direction. The charge of the primary quark or anti-quark in a hemisphere is necessary to determine the orientation of quark polar angle $\theta_{\vec{T}}$. This charge information can be obtained separately for both event hemispheres using the flavour tag Neural Network output.

4.2.1 Single and double hemisphere tagged events

In single hemisphere tagged events the orientation of the primary quark axis is obtained from the sign the Neural Net output. The quark axis is forward oriented ($\cos\theta_{\vec{T}} > 0$) if a forward hemisphere is tagged to contain a b quark or a backward hemisphere is tagged to contain a b anti-quark. Otherwise the quark axis is backward ($\cos\theta_{\vec{T}} < 0$) oriented.

One needs to distinguish two categories of events if both hemispheres are flavour tagged. The situation is similar to single hemisphere events, if one hemisphere is tagged as quark and the other as anti-quark. Here the event orientation is determined by either hemisphere, but the additional second hemisphere flavour tag increases the probability to correctly identify the quark charge. On the contrast, events for which both hemispheres are tagged to contain quarks (or both anti-quarks) do not have a preferred orientation. These like-sign events are used to measure the charge tagging probability.

4.2.2 The observed asymmetry

The difference of the number of forward and backward events normalised to the sum is related to the forward-backward asymmetry as can be seen from Equation 10. Thus for single hemisphere tag events:

$$A_{FB}^{obs} = \frac{N - \overline{N}}{N + \overline{N}} = \sum_{\mathrm{f=d,u,s,c,b}} (2 \cdot w_{\mathrm{f}} - 1) \cdot A_{FB}^{\mathrm{f}} \cdot p_{\mathrm{f}} \cdot \eta_{\mathrm{f}} \ , \tag{11}$$

where

$$\begin{array}{rcl} N & \sim & \text{number of single hemisphere tagged forward events,} \\ \overline{N} & \sim & \text{number of single hemisphere tagged backward events.} \end{array}$$

Similarly for the double hemisphere tagged events:

$$A_{FB}^{D,obs} = \frac{N^D - \overline{N^D}}{N^D + \overline{N^D}} = \sum_{\mathrm{f=d,u,s,c,b}} (2 \cdot w_{\mathrm{f}}^D - 1) \cdot A_{FB}^{\mathrm{f}} \cdot p_{\mathrm{f}}^D \cdot \eta_{\mathrm{f}} \ , \tag{12}$$

where

N^D $\sim$ number of double hemisphere tagged forward events,
$\overline{N^D}$ $\sim$ number of double hemisphere tagged backward events.

The observed asymmetry is the sum of the contributions from b events and from c and dus background events. A_{FB}^{f} is the forward-backward asymmetry, p_{f} and p_{f}^D are the purities for each flavour in the single and double tagged events categories. The η-term accounts for the differently signed charge asymmetries, $\eta_{\mathrm{f}} = 1$ for up-type quarks and $\eta_{\mathrm{f}} = -1$ for down-type quarks.

w_{f} and w_{f}^D are the probabilities to identify the quark charge correctly in single and double tagged events. For single tagged events:

$$w_{\mathrm{f}} = \frac{\hat{N}_{\mathrm{f}} + \hat{N}_{\overline{\mathrm{f}}}}{N_{\mathrm{f}} + N_{\overline{\mathrm{f}}}} \quad , \tag{13}$$

where $N_{\mathrm{f}}(N_{\overline{\mathrm{f}}})$ is the number of simulated events, which contain a quark (anti-quark) in the forward hemisphere. $\hat{N}_{\mathrm{f}}(\hat{N}_{\overline{\mathrm{f}}})$ is the number of events, in which the quark (anti-quark) has been correctly identified.

For unlike sign events the fraction of events, in which both quark and anti-quark charges are correctly identified, is defined analogously to the single hemisphere tagged events as the ratio of correctly tagged $(\hat{N}_{\mathrm{f}}^D, \hat{N}_{\overline{\mathrm{f}}}^D)$ over all double-tagged unlike-sign $(N_{\mathrm{f}}^D, N_{\overline{\mathrm{f}}}^D)$ events:

$$w_{\mathrm{f}}^D = \frac{\hat{N}_{\mathrm{f}}^D + \hat{N}_{\overline{\mathrm{f}}}^D}{N_{\mathrm{f}}^D + N_{\overline{\mathrm{f}}}^D} \quad . \tag{14}$$

To measure the b quark forward-backward asymmetry all quantities appearing in Equations 11 and 12 have to be determined. The rates N, $\overline{N}$, N^D, $\overline{N^D}$ are obtained from the data. The b purity, p_{b}, and the probability to correctly identify the b quark charge can also be extracted directly from data with only minimal input from simulation. The determination of p_{b} was discussed in section 3, the measurement of w_{b} and w_{b}^D are discussed in the next section. Only the small corrections for c and light quark backgrounds are based on simulation.

4.3 The probabilities to correctly identify the b quark charge

For the case of b quarks the probabilities to correctly identify the charge can be measured directly from the data leading to a self-calibration of the analysis. The principle idea of the method is that the unlike-sign and like-sign double tagged events are proportional to:

$$N^D + \overline{N^D} \propto [w_{\mathrm{b}}^2 + (1 - w_{\mathrm{b}})^2] \; , \tag{15}$$

$$N^{same} \propto 2 \cdot w_{\mathrm{b}} \cdot (1 - w_{\mathrm{b}}) \; . \tag{16}$$

where

N^{same} $\sim$ number of double tagged like-sign events.

Resolving the quadratic equations leads to:

$$w_{\mathrm{b}} \cdot \sqrt{1 + \delta} = \frac{1}{2} + \sqrt{\frac{1}{4} - \frac{1}{2} \cdot \frac{N^{same} \cdot p_{\mathrm{b}}^{same}}{[N^D + \overline{N^D}] \cdot p_{\mathrm{b}}^D + N^{same} \cdot p_{\mathrm{b}}^{same}}} \; , \tag{17}$$

$$w_{\mathrm{b}}^{D} \cdot \sqrt{1+\beta} = \frac{{w_{\mathrm{b}}}^2 \cdot (1+\delta)}{{w_{\mathrm{b}}}^2 \cdot (1+\delta) + (1 - w_{\mathrm{b}} \cdot \sqrt{1+\delta})^2} \ . \tag{18}$$

A detailed derivation of these equations can be found in the appendix. p_{b}^{D} and p_{b}^{same} are the b purities determined individually for the like-sign and unlike-sign categories using equations 3 and 4. The additional terms $\sqrt{1+\delta}$ and $\sqrt{1+\beta}$ allow for hemisphere charge correlations and are discussed in section 4.4.

In Figure 7 the measured probabilities for single and double tagged events are shown as a function of the polar angle for the year 1994. The results on data are corrected for tiny background contributions and are compared to the prediction from simulation. In double tagged events w_{b}^{D} is found to be above 92 % and drops to 87 % for large $\cos\theta_{\vec{T}}$ at the edge of the detector acceptance. A similar behaviour is found for the single tagged events. The tagging probabilities in simulation are found to be on average 2.5 % and 1.7 % higher for single and double tagged events, respectively.

4.4 The correlations δ and β

The probabilities to correctly identify the quark charge are deduced from double hemisphere tagged like-sign and unlike-sign events. Correlations between the two hemisphere charges in different event categories affect the measurement and need to be taken into account. The term $\sqrt{1+\delta}$ in Equation 17 allows for such correlations when calculating the single tagged probability, w_{b} , using the double tagged events. The probability to identify the quark charge in double tagged unlike-sign events, w_{b}^{D} , is obtained from w_{b} using Equation 18. Here the additional term $\sqrt{1+\beta}$ allows for the different correlations in double tagged unlike-sign events.

The correlation terms $\sqrt{1+\delta}$ and $\sqrt{1+\beta}$ are obtained from simulation using b quark events. The result of the right side of Equation 17 can be compared to the true tagging probability for single tagged events calculated using the simulation truth. The ratio of both results is given by the term $\sqrt{1+\delta}$. Similarly the term $\sqrt{1+\beta}$ is deduced from the ratio of the result from the right side of Equation 18 and the truth in double tagged unlike-sign events. In Figure 8 the correlations δ (upper plot) and β (lower plot) are shown as a function of the polar angle $\cos\theta_{\vec{T}}$ for the different years of data taking. At the working point the average correlations are $\langle\delta\rangle = 0.0552 \pm 0.0027$ and $\langle\beta\rangle = 0.0343 \pm 0.0018$. Within errors the correlations are stable as a function of the polar angle up to the end of the acceptance. No significant variation is found between the years.

Possible sources of the hemisphere charge correlation have been investigated in detail. In order to understand the origin of the correlations experimental input variables where consecutively discarded from the flavour tagging Neural Network. With these modified flavour tagging the measurement was repeated. Only for the flavour network for which the jet charges for $\kappa = 0.3$ and $\kappa = 0.6$ were omitted a significant variation in the correlation is observed. The mean of the correlations $\langle\delta\rangle$ and $\langle\beta\rangle$ calculated with this flavour tag are shown as dashed lines in Figure 9. This can be compared to the dependence of the correlation for the full Neural Network as a function of the cut on the flavour tag output $|flav_{\mathrm{hem}}|$, which is shown as points. Nearly no correlation remains for $\langle\delta\rangle$ and only a small correlation for $\langle\beta\rangle$ after removing the jet charge information.

The composition of events in the single and double tagged categories are changed when removing the jet charge from the network input. More three jet like events survive the cut on $|flav_{\mathrm{hem}}|$ for the full flavour tag Neural Network including jet charge information.

Also, events are more two jet like with increasing values for the cut on $|flav_{\rm hem}|$. This behaviour is illustrated by applying a cut on the thrust value of $|\vec{T}| > 0.9$ to the events before entering both versions of the Network, which is also shown in Figure 9. Hence the hemisphere charge correlations δ and β are sensitive to gluon radiation.

The source of hemisphere charge correlations for the jet charge analysis has been studied in reference [4]. It was found that the dominant source of correlations are QCD effects introduced by gluon radiation. The same behaviour is found for the flavour tagging Neural Network using this information.

Further possible sources of correlations have been investigated. The beam spot is shifted with respect to the centre of the DELPHI detector. Furthermore its dimension differs in x and y by more than one order of magnitude. A possible ϕ structure in the mean correlations $\langle\delta\rangle$ and $\langle\beta\rangle$ have been investigated comparing results for different intervals of the thrust azimuthal angle, $\phi_{\vec{T}}$. No significant variation has been found.

5 The measurement of $A_{FB}^{\rm b}$

The differential asymmetry is insensitive to changes in the detector efficiency between different bins in polar angle. Hence the measurement of the b asymmetry is done in nine consecutive intervals of $\cos\theta_{\vec{T}}$. In each bin the observed asymmetry is given by replacing in Equations 11 and 12 the b quark forward-backward asymmetry, $A_{FB}^{\rm b}$, by the differential asymmetry:

$$A_{FB}^{\rm b,diff}(\cos\theta_{\vec{T}}) \;=\; \frac{8}{3}\cdot A_{FB}^{\rm b}\cdot\frac{\cos\theta}{1+\cos\theta}\;. \tag{19}$$

To extract $A_{FB}^{\rm b}$ all parameters of Equations 11 and 12 need to be determined bin by bin. The probabilities $w_{\rm b}$ and $w_{\rm b}^D$ to correctly identify the b quark charge as a function of the polar angle were discussed above. This includes corrections for the hemisphere correlations for each bin.

After the complete selection the combined data sample of single and unlike-sign double flavour tagged events contains a b fraction, $p_{\rm b}$, of close to 94%. In Figure 10 the $\cos\theta_{\vec{T}}$ dependence of the b purities $p_{\rm b}$ and $p_{\rm b}^D$ and of the b efficiencies $\epsilon_{\rm b}$ and $\epsilon_{\rm b}^D$ are shown. The data is compared to the simulation. Both, the efficiency and the purity are stable in the central region of the detector. At large $\cos\theta_{\vec{T}}$ the purity increases slowly for both categories of single and double tagged events. At the same time the b efficiency decreases with a fast drop for $\cos\theta_{\vec{T}} > 0.7$. This effect is due to a decreasing detector performance for the b tagging causing only events with a clear b signature to be tagged. The simulation reproduces the shape of the data.

Small corrections for c and light quark backgrounds in Equations 11 and 12 are estimated from simulation. For all non-b flavour the probability of identifying the quark charge correctly is calculated in each bin from the simulation using Equation 13 for the single tagged and Equation 14 for the double tagged events. The corresponding purities are estimated based on the efficiencies from simulation using Equation 4.

The background forward-backward asymmetries for d , u and s quark events are set to the Standard Model values and for c events the forward-backward asymmetry is set to its measured LEP value ($A_{FB}^{\rm c} = 0.0689 \pm 0.0035$) [3].

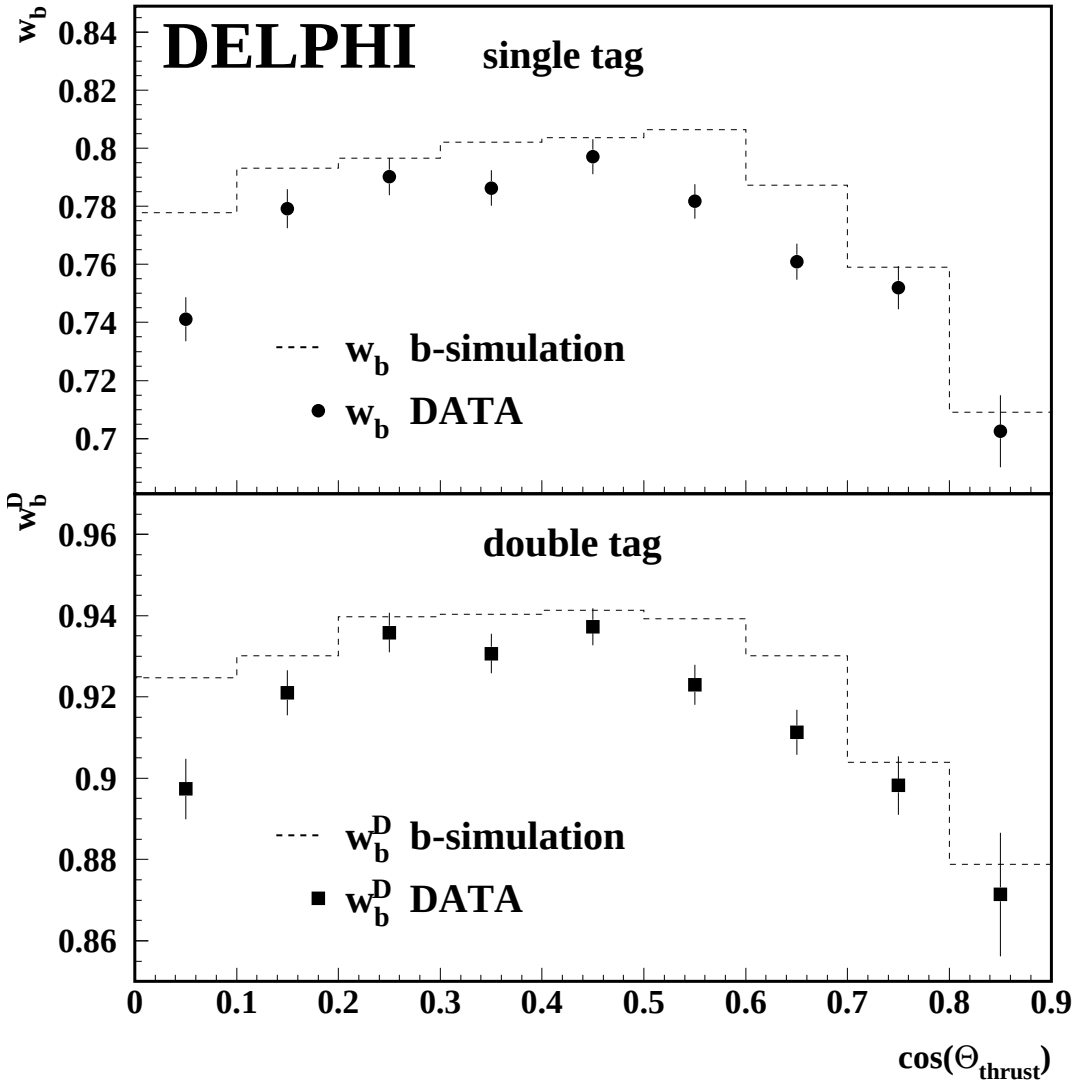

Figure 7: *The probability to correctly identify b quarks for data and simulation for the year 1994. The upper plot shows the result for single tagged events, the lower for double tagged events. See text for details.*

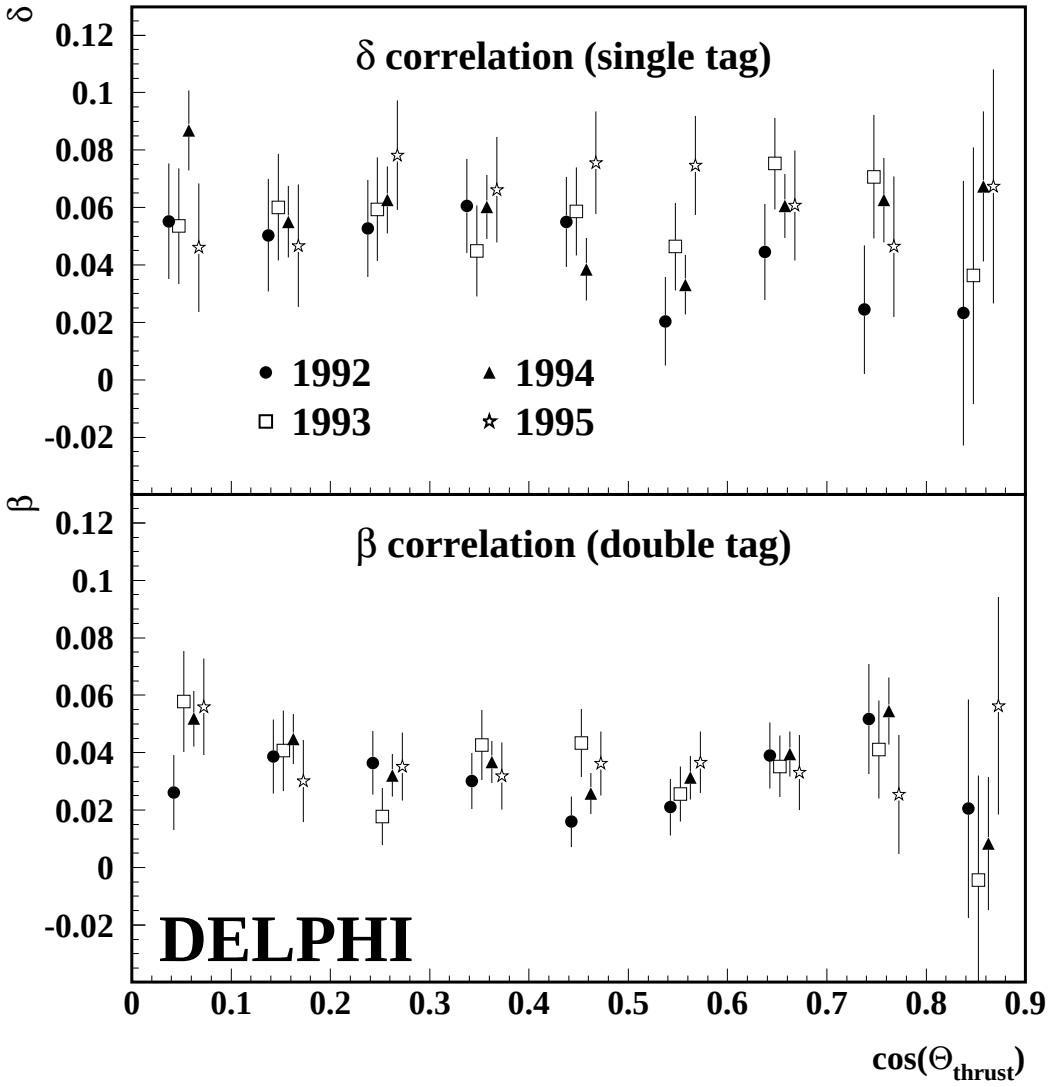

Figure 8: *Correlation of single and double tagged events of the years 1992 to 1995.*

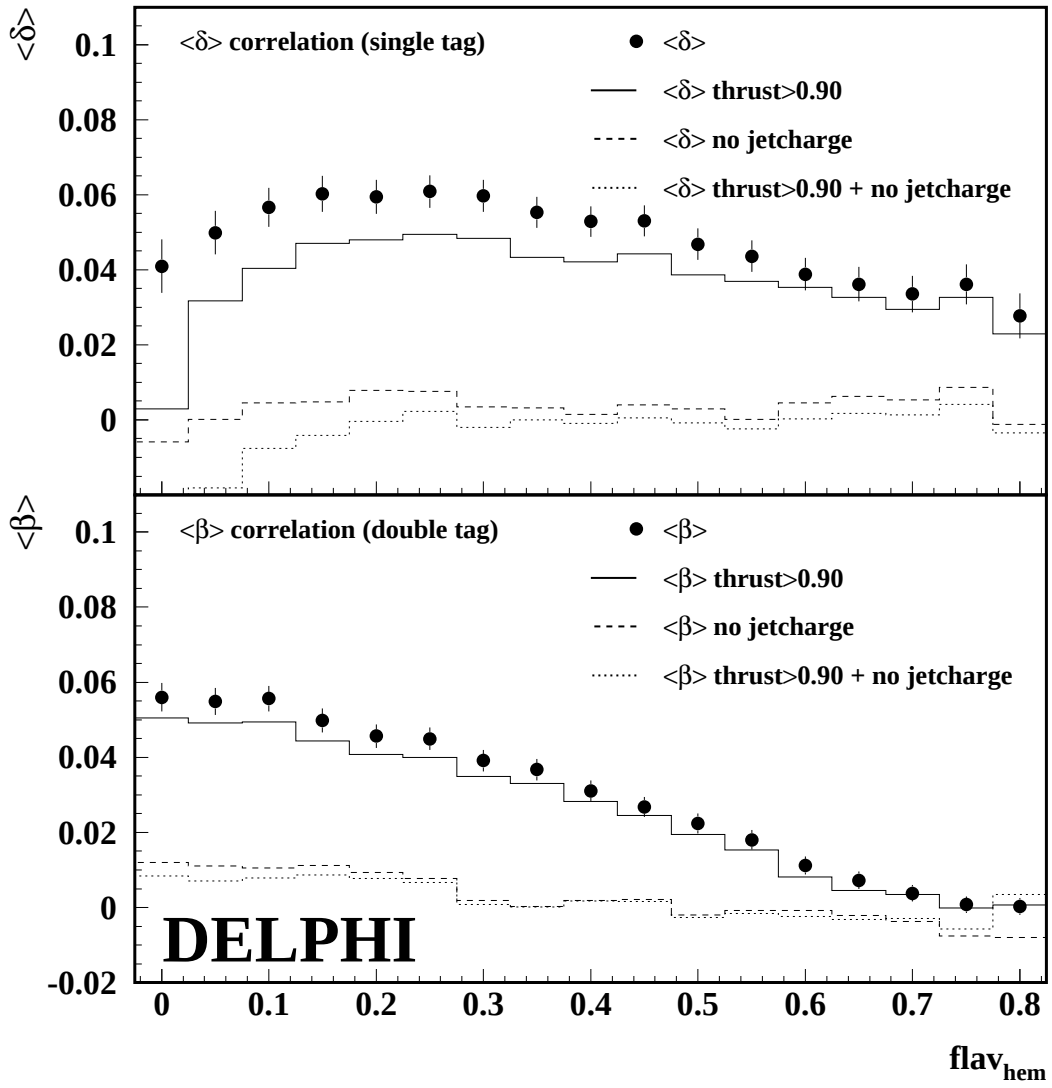

Figure 9: *The mean of the correlations δ and β of 1994 simulation in dependence of the cut on the flavour tag output $|flav_{hem}|$. Besides the full flavour network (points) results using modified flavour networks without the jet charge input and both with an additional cut on the thrust value, $|\vec{T}| > 0.9$, are shown.*

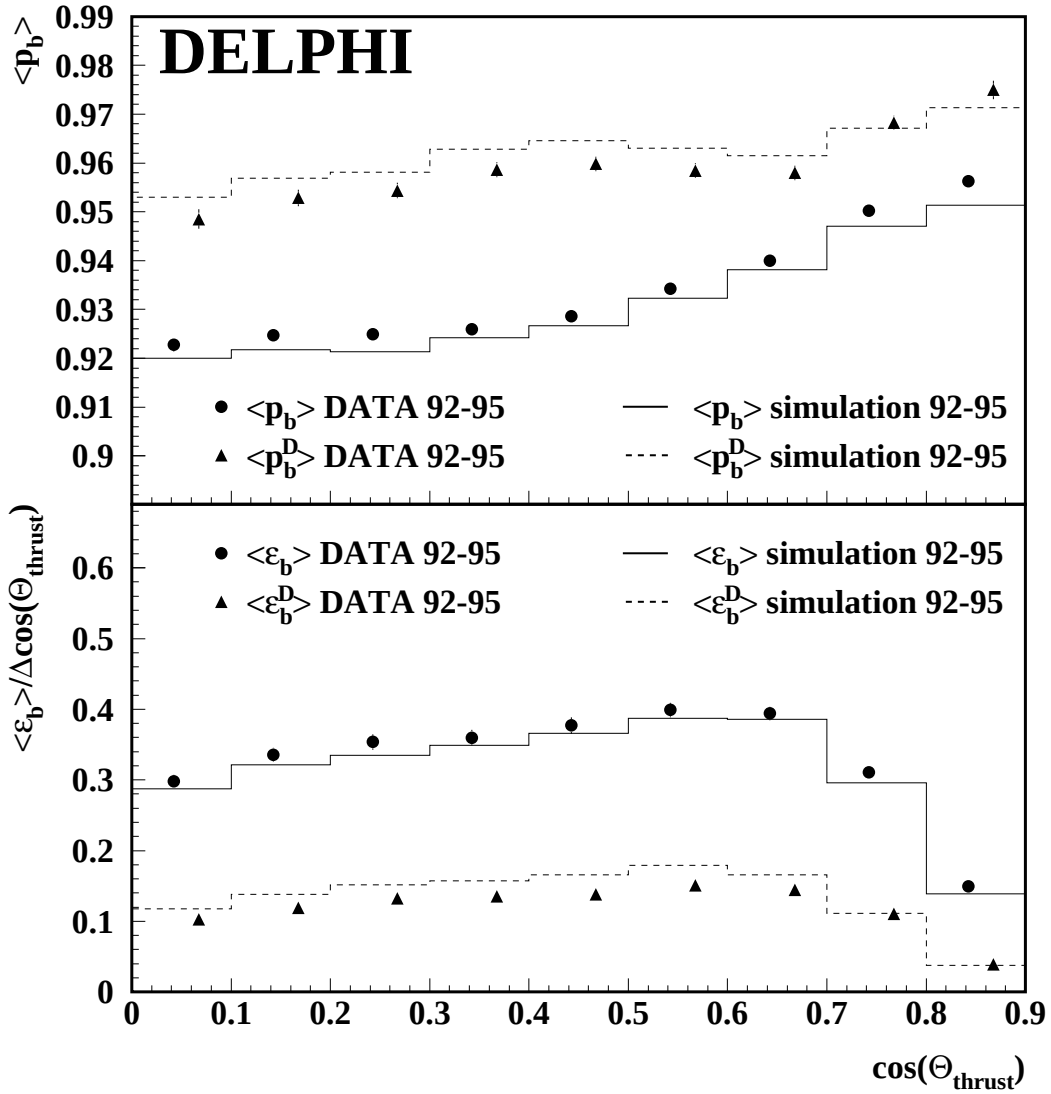

Figure 10: *The b purities $p_{\rm b}$ and $p_{\rm b}^D$ and the efficiencies $\epsilon_{\rm b}$ and $\epsilon_{\rm b}^D$ for single and double tagged events as a function of the polar angle.*

5.1 The QCD correction

The measurement of the b quark forward-backward asymmetry is sensitive to QCD corrections to the quark final state. These corrections are know up to the 2nd order for massless quarks for a measurement using the thrust axis to approximate the initial quark direction.

A realistic measurement has a reduced experimental sensitivity to the QCD effects because of biases in the analysis against events with hard gluon radiation. In this analysis the flavour tagging and also the b tagging introduces a bias against QCD effects. Therefore the QCD correction can be written as [15]:

$$A_{FB}^{\mathrm{b},QCD} = (1 - C_{\mathrm{b}})A_{FB}^{\mathrm{b},noQCD} = (1 - s_{\mathrm{b}}\, C_{QCD}^{\mathrm{b}})A_{FB}^{\mathrm{b},noQCD}. \tag{20}$$

Here $A_{FB}^{\mathrm{b},noQCD}$ is the asymmetry of the initial b quarks without gluon radiation, which can be calculated from the measured asymmetry $A_{FB}^{\mathrm{b},QCD}$ through the correction coefficient C_{b}. This correction coefficient is given by the product of a bias factor s_{b}, which accounts for the sensitivity of the individual analysis to the QCD correction C_{QCD}^{b}, and of C_{QCD}^{b}, which is the QCD correction to the b quark forward-backward asymmetry measured using the thrust direction. The value of the QCD correction is estimated to be [16]:

$$C_{QCD}^{\mathrm{b}} = (3.54 \pm 0.63)\% \tag{21}$$

The experimental bias is studied on simulation by fitting the differential asymmetry of the b simulation after setting the generated asymmetry of the initial b quarks before gluon radiation to the maximum of 75%. The observed relative differences of the asymmetries are studied separately for each $\cos\theta_{\vec{T}}$ interval. In Figure 11 the coefficient C_{b} is shown for single and double tagged events for the different years. At small polar angle the sensitivity to the asymmetry is small and hence C_{b} receives a larger statistical uncertainty. No clear systematic variation is seen at large polar angles.

year	C_{b} [%]	s_{b} [%]
1992	0.58 ± 0.25	19 ± 8
1993	0.65 ± 0.23	21 ± 8
1994	0.34 ± 0.29	11 ± 10
1995	0.55 ± 0.36	18 ± 12

Table 5: Summary of coefficients C^{b} and bias factors s_{b} with their statistical uncertainty.

From the coefficient C_{b} the experimental bias factor s_{b} is deduced. The averaged values of C_{b} and s_{b} are shown in Table 5 for the different years of data taking. In the following the correction coefficients C_{b} are taken into account for each bin in polar angle separately and hence all asymmetries quoted are corrected for QCD effects.

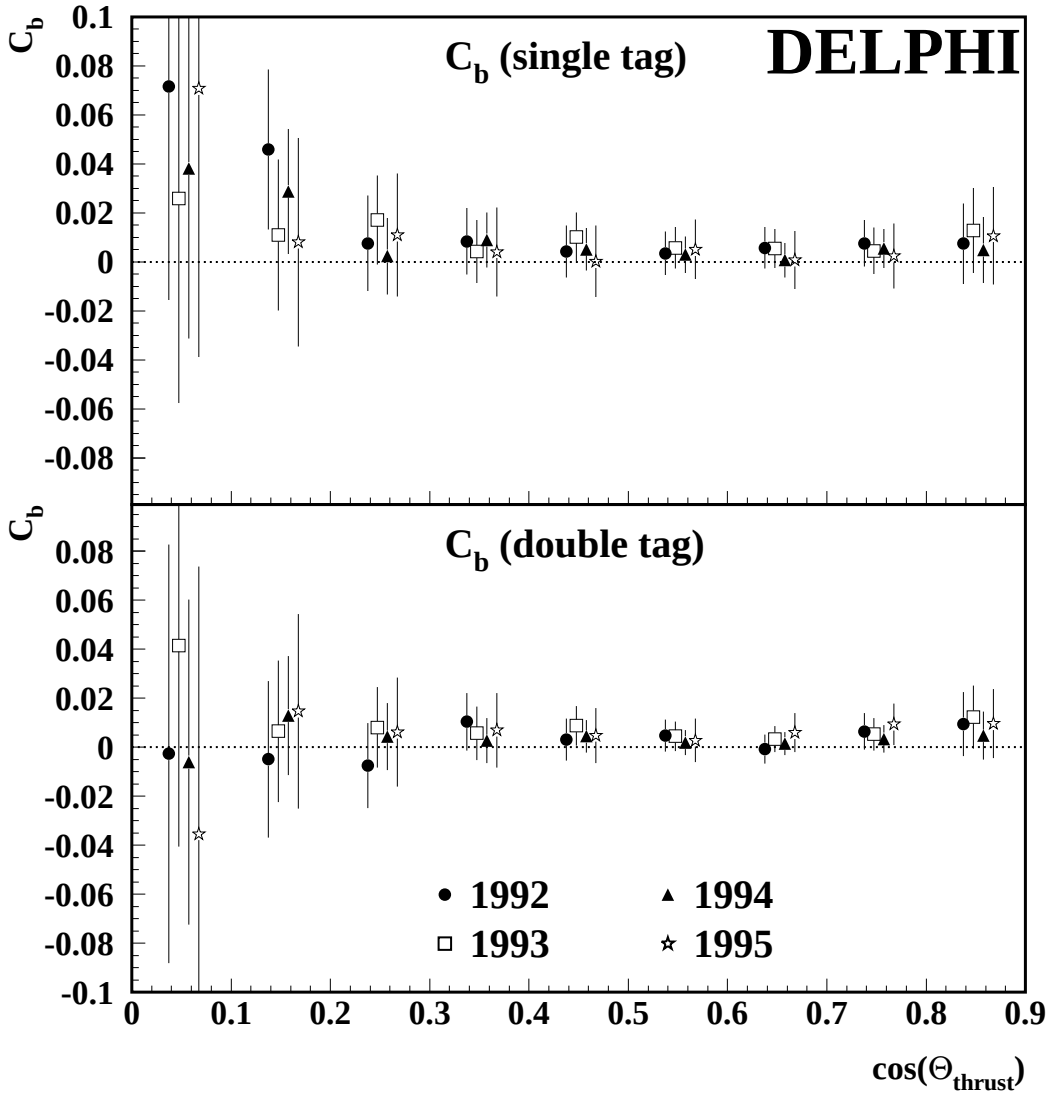

Figure 11: *The size of the QCD correction including experimental biases as a function of the polar angle of the thrust axis. In the upper plot the correction is shown for single tagged events from the different years. In the lower plot the corresponding corrections are shown for double tagged events.*

5.2 The fit of the b quark forward-backward asymmetry

Technically the b quark forward-backward asymmetry A_{FB}^{b} is extracted from a χ^2-fit to the five independent event categories N, $\overline{N}$, N^D, $\overline{N^D}$and N^{same} in bins of polar angle. The double hemisphere tagged unlike-sign events are sensitive to the asymmetry, but the rates also enter into the determination of the charge tagging probabilities w_{b} and w_{b}^D , as can be seen in Equations 17 and 18. This leads to correlations between the probabilities and the measured asymmetry in each bin.

In the combined χ^2-fit to the five events rates N, $\overline{N}$, N^D, $\overline{N^D}$and N^{same} these correlations are taken into account. Using the equations above the rates can be expressed as a function of the b quark forward-backward asymmetry A_{FB}^{b}, the probability w_{b} and two arbitrary normalisation factors which absorb the overall efficiency corrections.

Figure 12 shows the measured differential asymmetry for single and double tagged events as a function of $\cos\theta_{\vec{T}}$ averaged over all years of data taking. Only statistical errors are shown. The band represents the overall result. The summary of the individual A_{FB}^{b} results for the different years with their statistical uncertainties is given in Table 6.

year	$\sqrt{s}$ [GeV]	A_{FB}^{b}	χ^2/ndf
1992	91.280	0.0915 ± 0.0077	0.54
1993	91.225	0.0997 ± 0.0094	0.84
1994	91.202	0.0935 ± 0.0047	0.88
1995	91.288	0.0849 ± 0.0084	1.04

Table 6: Summary of the A_{FB}^{b} results for the different years with their statistical error. The number of degrees of freedom is 17 for the fit of each year of data taking.

Figure 13 shows the average b quark forward-backward asymmetry, A_{FB}^{b}, as a function of the cut on the flavour tag Neural Netword output $flav_{\mathrm{hem}}$ and the expected total error from the simulation. The black point represents the chosen working point of this analysis, which minimises the total expected error.

Combining these measurements taking common uncertainties into account yields the final result:

$$A_{FB}^{\mathrm{b}}\ (91.26\ \mathrm{GeV}) \quad = \quad 0.0931 \pm 0.0034(\mathrm{stat.}) \quad .$$

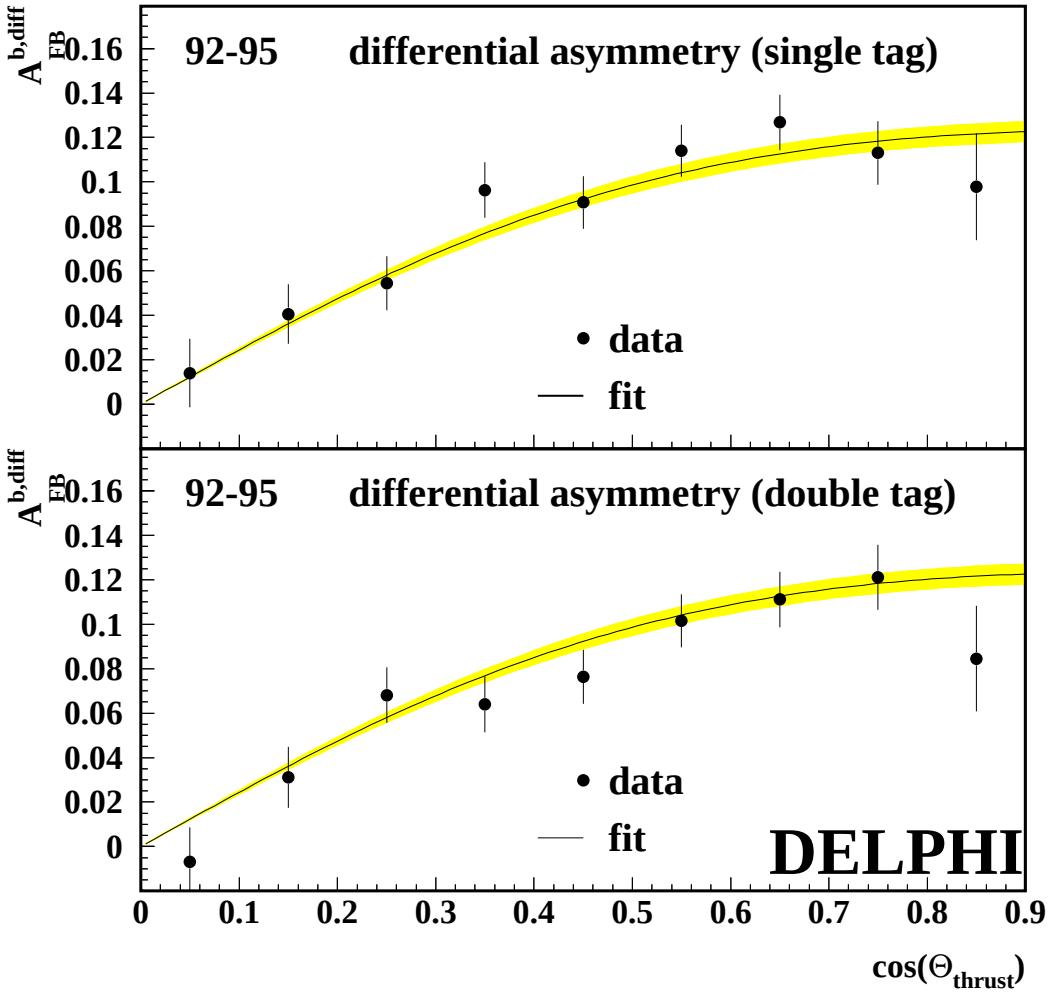

Figure 12: *The differential b quark forward-backward asymmetry of the years 1992 to 1995. The line is the result of the χ^2-fit with its statistical error shown as the band.*

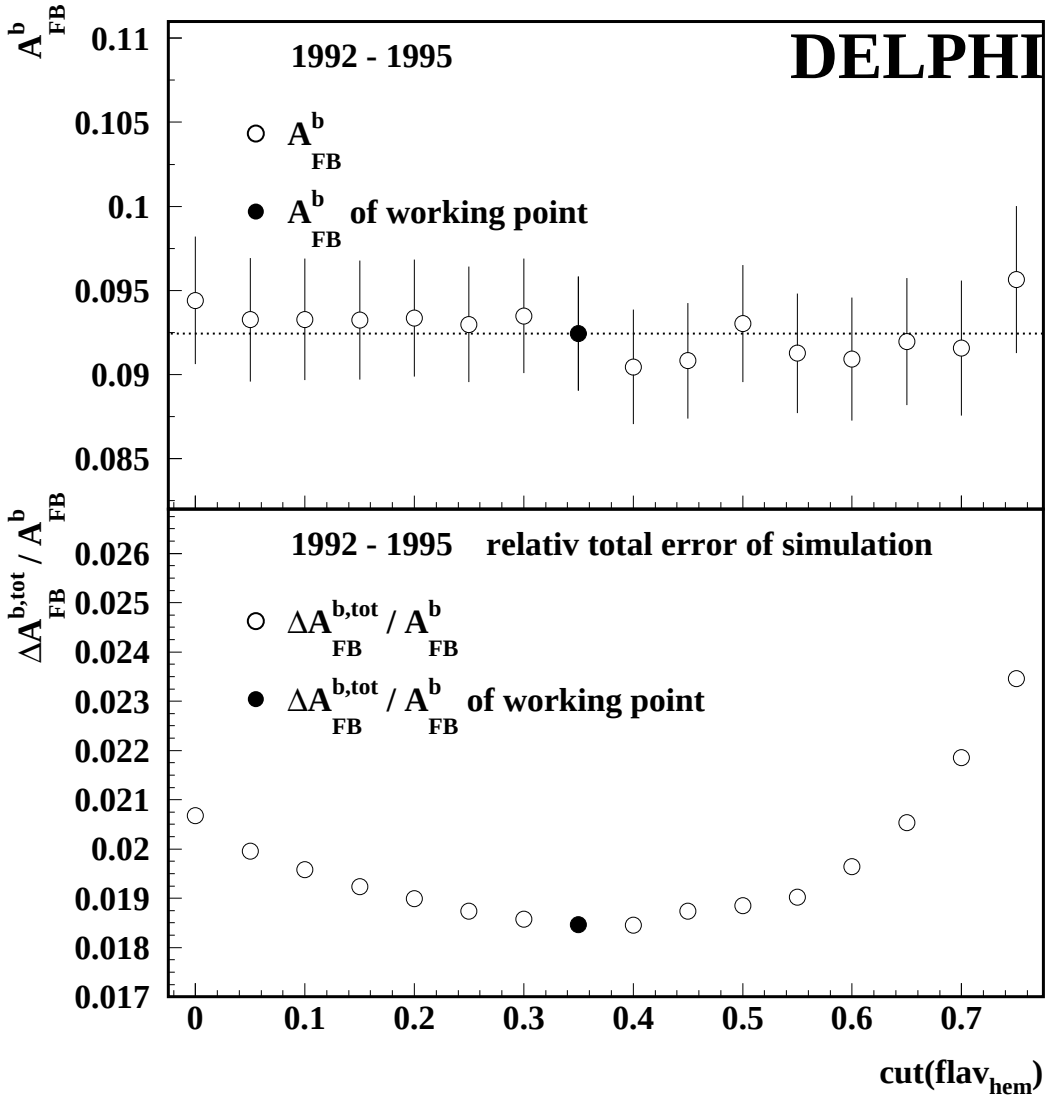

Figure 13: *The average A^{b}_{FB} result and its statistical uncertainty in dependence on the cut variable $|flav_{hem}|$ for all years of data taking (upper plot). The expected total error from the simulation (lower plot). The values at working point are shown as black points.*

6 Discussion of systematic uncertainties

Systematic uncertainties introduced by the b tagging

The measurement of the purity, p_{b}, and of the efficiency, ϵ_{b}, of the lifetime b tagging is affected by systematic uncertainties of the input quantities entering in Equation 4. The variations of these input quantities are studied and changes in the result are propagated through the whole analysis chain.

R_{c} and R_{b} are set to the LEP average values $R_{\mathrm{c}} = 0.1709 \pm 0.0034$ and $R_{\mathrm{b}} = 0.21653 \pm 0.00069$ [3]. A variation of $\pm 3\%$ on R_{c} and of $\pm 0.35\%$ on R_{b} is included in the systematic error.

The uncertainties on efficiencies of the light and c quark background due to the modelling are studied by varying the relevant parameters in the simulation. The light quark efficiency ϵ_{uds} is sensitive to:

- Gluon splitting into $\mathrm{c\bar{c}}$ pairs or $\mathrm{b\bar{b}}$ pairs in light quark events give rise to lifetime information from the decays of the produced heavy quark hadrons. A variation of the splitting rates within the present world averages $g \to c\bar{c} = 3.19 \pm 0.46\%$ [17] and $g \to b\bar{b} = 0.251 \pm 0.063\%$ [18] is included in the systematic error.

- Decays of K^0 and Λ in flight lead to tracks with large impact parameters w.r.t. the primary vertex and consequently can lead to a lifetime tag of the event. The rate of such decays in light quark events was varied by $\pm 10\%$ to estimate the effect on the light quark efficiency ϵ_{uds} .

The systematic error sources on ϵ_{c} are:

- The relative production fractions of the different c hadron type in c events is an important source of systematic uncertainty for the b tagging because of the huge difference in the average lifetimes. Following the prescription in reference [19] the rates of D^+, $\mathrm{D_s}$ and c baryons per c quark event are varied individually keeping the total sum constant. The changes are compensated by a shift of the D^0 fraction. The present world averages are listed in Table 7.

- The c hadron lifetimes are varied within the errors given in Table 7 to estimate the affects on the b tagging.

- c hadrons produced in the fragmentation of c quarks carry a large fraction of the initial quark energy. The influence of the uncertainty of the average scaled momentum $\langle x_E \rangle$ of c hadrons in c events is studied by reweighting the events such that the resulting $\langle x_E \rangle$ changes by $\pm 2\%$ corresponding to the uncertainty of the measurement 0.480 ± 0.008 [19].

- The b tagging efficiency of c events is sensitive to the average charged multiplicity of c decays. The multiplicities are varied according to the inclusive topological branching ratios measured for D^0 ($2.56 \pm 0.04 \pm 0.03$), D^+ ($2.38 \pm 0.04 \pm 0.05$) and $\mathrm{D_s}$($2.69 \pm 0.31 \pm 0.1$) [20].

D meson	fraction	lifetime $[ps]$
D^0	0.600	0.415 ± 0.004
D^+	0.233 ± 0.027	1.057 ± 0.015
D_s	0.102 ± 0.029	0.447 ± 0.017
c baryons	0.063 ± 0.028	0.206 ± 0.012

Table 7: D meson and b baryon fractions and lifetimes.

Systematic uncertainties on the charge tagging

The hemisphere charge correlations and the corrections for c and light background are the dominant sources of systematic error on the charge tagging. The statistical uncertainty of the charge tagging probabilities $w_{\rm b}$ and $w_{\rm b}^D$ are determined in the χ^2-fit and are included in the statistical error on $A_{FB}^{\rm b}$.

The source of the hemisphere charge correlations δ and β are discussed in section 4.4. The uncertainty of the QCD effects giving rise to the hemisphere correlations in the jet charge were estimated in reference [4] to be ~ 20 % of the total correction. It has been checked that the relative weight of the jet charge information in the Neural Net is similar in data and simulation. No additional uncertainty is added to the systematic error.

The uncertainty on the charge identification probabilities $w_{\rm f}$ and $w_{\rm f}^D$ for c and light quark background events affect the measurement. The dominant background contribution is due to c events. Systematic effects on $w_{\rm c}$ and $w_{\rm c}^D$ due to the modelling of the c hadron production and decay in c events are included in the variation of fragmentation parameters discussed above. An additional $\pm 10\%$ variation of $w_{\rm f}$ and $w_{\rm f}^D$ for c and light quark events is added to the systematic error to account for imperfections of the fragmentation model and uncertainties of the parameter tuning as well as in the simulation of the detector response.

The simulation has been corrected, in a similar fashion as for the tuning of the impact parameter b tagging, to better describe the performance of the flavour tagging in data. A reweighting method is used to correct for small disagreements in the particle impact parameter quality information and in the number of accepted tracks per hemisphere entering the flavour tagging Neural Network. Using different reweighting functions leads to small systematic variations of the measured asymmetry of the order of 0.07 %.

Systematic uncertainties due to other effects

- The forward-backward asymmetry of c events has been taken from the LEP value ($A_{FB}^{\rm c} = 0.0689 \pm 0.0035$) [3]. Within the analysis this $A_{FB}^{\rm c}$ value has been varied by 5%.

- The contribution to the total error due the limited Monte Carlo sample can be estimated by dropping from the χ^2-fit the statistical uncertainties from the simulation. It is quoted separately from the pure statistical error of the data.

- The uncertainty on the QCD correction receives contributions from the theoretical prediction [15] and from the estimation of the experimental bias factors.

- The b efficiencies, purities and the flavour tagging probabilities are all calibrated from data. It has been checked that the measurement is insensitive to systematic variations of the b fragmentation and to the B fractions and lifetimes.

All contributions to the systematic error are summarised separately for each year in Table 8.

Contribution	Variation	$\Delta A_{FB}^{\mathrm{b}} \times 10^2$
		$\sum$ 92-95
R_{b}	$\mp 0.35\%$	± 0.0009
R_{c}	$\pm 3\%$	± 0.003
A_{FB}^{c}	$\pm 5\%$	± 0.021
statistical error of simulation		± 0.019
reweighting of simulation		± 0.006
error of QCD correction		± 0.027
identification probabilities $w_{\mathrm{u,d,s,c}}$	$\pm 10\%$	± 0.069
hemisphere correlations δ, β	$\pm 20\%$	∓ 0.080
Detector resolution		± 0.100
Gluon splitting $g \to \mathrm{c\bar{c}}$	$\pm 0.46\%$	± 0.005
Gluon splitting $g \to \mathrm{b\bar{b}}$	$\pm 0.063\%$	± 0.003
K^0,Λ variation	$\pm 10\%$	± 0.007
D^+ fraction in $\mathrm{c\bar{c}}$	0.233 ± 0.027	± 0.053
$\mathrm{D_s}$ fraction in $\mathrm{c\bar{c}}$	0.102 ± 0.029	± 0.041
c baryon fraction in $\mathrm{c\bar{c}}$	0.063 ± 0.028	∓ 0.014
c hadron lifetimes	see Tab. 7	∓ 0.007
D decay multiplicity	see Tab. 7	± 0.003
$\langle x_E \rangle_{\mathrm{c}}$ (fragmentation)	$\pm 2\%$	∓ 0.015

Table 8: Systematic uncertainties and their influence on the determination of A_{FB}^{b}.

7 Conclusions

This measurement of A_{FB}^{b} uses an enhanced impact parameter b tagging and an inclusive quark flavour tagging Neural Network. The analysis is based on the LEP 1 data collected with the DELPHI detector from 1992 up to 1995. The measured b quark forward-backward asymmetries for the individual years of data taking are:

$$\begin{array}{lrcl} 1992\ (91.280\ \mathrm{GeV}): & A_{FB}^{\mathrm{b}} & = & 0.0915 \pm 0.0077(\mathrm{stat.}) \\ 1993\ (91.225\ \mathrm{GeV}): & A_{FB}^{\mathrm{b}} & = & 0.0997 \pm 0.0094(\mathrm{stat.}) \\ 1994\ (91.202\ \mathrm{GeV}): & A_{FB}^{\mathrm{b}} & = & 0.0935 \pm 0.0047(\mathrm{stat.}) \\ 1995\ (91.288\ \mathrm{GeV}): & A_{FB}^{\mathrm{b}} & = & 0.0849 \pm 0.0084(\mathrm{stat.}) \end{array}$$

These measurements are QCD corrected. The final result is obtained taking correlated systematic errors into account:

$$A_{FB}^{\mathrm{b}}\ (91.26\ \mathrm{GeV}) \quad = \quad 0.0931 \pm 0.0034(\mathrm{stat.}) \pm 0.0017(\mathrm{syst.}) \quad .$$

From this measurement the b quark pole asymmetry is extracted. Corrections for QED, photon exchange and γZ interference amount to 0.0041 and -0.0003, respectively. A correction of -0.0013 is applied to correct for the energy dependence of the asymmetry. This yields:

$$A_{FB}^{0,\mathrm{b}} \quad = \quad 0.0956 \pm 0.0038 \quad .$$

Using equation 2 one obtains for the effective electroweak mixing angle $\sin^2\theta_{\mathrm{eff}}^{\ell}$:

$$\sin^2\theta_{\mathrm{eff}}^{\ell} \quad = \quad 0.23287 \pm 0.00068$$

The measurement presented in this paper agrees well with previous determinations of $\sin^2\theta_{\mathrm{eff}}^{\ell}$ at LEP and consequently with the LEP avarage value. The results represents the most precise single measurement of $\sin^2\theta_{\mathrm{eff}}^{\ell}$ based on the b quark forward-backward asymmetry measurements of LEP [22, 4, 23, 24, 25, 26, 27, 28]. It improves by 25 % on the precision w.r.t. the previous results.

However, the analysis yields a result which is about three standard deviations higher than the measurement of the effective electroweak mixing angle obtained from the left-right cross section asymmetry by SLD [29].

Acknowledgements

We are greatly indebted to our technical collaborators, to the members of the CERN-SL Division for the excellent performance of the LEP collider and to the funding agencies for their support in building and operating the DELPHI detector.
We acknowledge in particular the support of
Austrian Federal Ministry of Education, Science and Culture, GZ 616.364/2-III/2a/98,
FNRS–FWO, Flanders Institute to encourage scientific and technological research in the industry (IWT), Belgium,
FINEP, CNPq, CAPES, FUJB and FAPERJ, Brazil,
Czech Ministry of Industry and Trade, GA CR 202/96/0450 and GA AVCR A1010521,
Commission of the European Communities (DG XII),
Direction des Sciences de la Matière, CEA, France,
Bundesministerium für Bildung, Wissenschaft, Forschung und Technologie, Germany,
General Secretariat for Research and Technology, Greece,
National Science Foundation (NWO) and Foundation for Research on Matter (FOM), The Netherlands,
Norwegian Research Council,
State Committee for Scientific Research, Poland, 2P03B06015, 2P03B11116 and SPUB/P03/DZ3/99,
JNICT–Junta Nacional de Investigação Científica e Tecnológica, Portugal,
Vedecka grantova agentura MS SR, Slovakia, Nr. 95/5195/134,
Ministry of Science and Technology of the Republic of Slovenia,
CICYT, Spain, AEN96–1661 and AEN96-1681,
The Swedish Natural Science Research Council,
Particle Physics and Astronomy Research Council, UK,
Department of Energy, USA, DE–FG02–94ER40817.

Appendix

In this measurement five events are selected in five different categories. These categories are defined in section 4.2:

N	$\sim$	number of single hemisphere tagged forward events,
$\overline{N}$	$\sim$	number of single hemisphere tagged backward events,
N^D	$\sim$	number of double hemisphere tagged forward events,
$\overline{N^D}$	$\sim$	number of double hemisphere tagged backward events,
N^{same}	$\sim$	number of double tagged like-sign events.

w_f and w_f^D are the probabilities to identify the quark charge correctly in single and double tagged events. For single tagged events it is defined as:

$$w_\mathrm{f} = \frac{\hat{N}_\mathrm{f}}{N_\mathrm{f}} = \frac{\hat{N}_{\overline{\mathrm{f}}}}{N_{\overline{\mathrm{f}}}} \; , \tag{22}$$

where $N_\mathrm{f}(N_{\overline{\mathrm{f}}})$ is the number of events, which contain a quark (anti-quark) in the forward hemisphere. $\hat{N}_\mathrm{f}(\hat{N}_{\overline{\mathrm{f}}})$ is the number of events, in which the quark (anti-quark) has been correctly identified. It has been checked on simulation that the tagging efficiencies are equal for quarks and anti-quarks.

For unlike sign events the fraction of events, in which both quark and anti-quark charges are correctly identified, is defined analogously to the single hemisphere tagged events as the ratio of correctly tagged $(\hat{N}_\mathrm{f}^D, \hat{N}_{\overline{\mathrm{f}}}^D)$ over all double-tagged unlike-sign $(N_\mathrm{f}^D, N_{\overline{\mathrm{f}}}^D)$ events:

$$w_\mathrm{f}^D = \frac{\hat{N}_\mathrm{f}^D}{N_\mathrm{f}^D} = \frac{\hat{N}_{\overline{\mathrm{f}}}^D}{N_{\overline{\mathrm{f}}}^D} \; . \tag{23}$$

The single and double tagged unlike- and like-sign samples receive contributions from b events and from all other flavours. All categories also include events for which the quark charge was misidentified. Therefore the number of events entering in the different categories can be expressed as:

$$N = \sum_{\mathrm{f=d,s,b}} [N_\mathrm{f} \cdot w_\mathrm{f} + N_{\overline{\mathrm{f}}} \cdot (1 - w_\mathrm{f})] + \sum_{\mathrm{f=u,c}} [N_{\overline{\mathrm{f}}} \cdot w_\mathrm{f} + N_\mathrm{f} \cdot (1 - w_\mathrm{f})] \tag{24}$$

$$\overline{N} = \sum_{\mathrm{f=d,s,b}} [N_{\overline{\mathrm{f}}} \cdot w_\mathrm{f} + N_\mathrm{f} \cdot (1 - w_\mathrm{f})] + \sum_{\mathrm{f=u,c}} [N_\mathrm{f} \cdot w_\mathrm{f} + N_{\overline{\mathrm{f}}} \cdot (1 - w_\mathrm{f})] \tag{25}$$

$$N^D = \sum_{\mathrm{f=d,s,b}} [N_\mathrm{f}^D \cdot w_\mathrm{f}^D + N_{\overline{\mathrm{f}}}^D \cdot (1 - w_\mathrm{f}^D)] + \sum_{\mathrm{f=u,c}} [N_{\overline{\mathrm{f}}}^D \cdot w_\mathrm{f}^D + N_\mathrm{f}^D \cdot (1 - w_\mathrm{f}^D)] \tag{26}$$

$$\overline{N^D} = \sum_{\mathrm{f=d,s,b}} [N_{\overline{\mathrm{f}}}^D \cdot w_\mathrm{f}^D + N_\mathrm{f}^D \cdot (1 - w_\mathrm{f}^D)] + \sum_{\mathrm{f=u,c}} [N_\mathrm{f}^D \cdot w_\mathrm{f}^D + N_{\overline{\mathrm{f}}}^D \cdot (1 - w_\mathrm{f}^D)] \tag{27}$$

$$N^{same} = \sum_{\mathrm{f=d,u,s,c,b}} N_\mathrm{f}^{same} \tag{28}$$

Here N_f ($N_{\overline{\mathrm{f}}}$) denominates the number of single tagged events containing a quark (anti-quark) of flavour f in the forward hemisphere. Similarly N_f^D ($N_{\overline{\mathrm{f}}}^D$) is the number of

unlike-sign double tagged events containing a quark (anti-quark) of flavour f in the forward hemisphere. N_{f}^{same} is the number of like-sign double tagged events for each flavour.

Assuming a data sample which contains only b quark events w_{b} can be extracted from the double tagged event samples. The sum of the unlike-sign double tagged events and the number of like-sign events is related to w_{b} :

$$N^D + \overline{N^D} = \left(N^D + \overline{N^D} + N^{same}\right) \cdot [w_{\mathrm{b}}^2 + (1 - w_{\mathrm{b}})^2] \quad (29)$$

$$N^{same} = 2 \cdot \left(N^D + \overline{N^D} + N^{same}\right) \cdot w_{\mathrm{b}} \cdot (1 - w_{\mathrm{b}}) \quad (30)$$

Both equations are linked through the total number of double tagged events and therefore contain the same information. Resolving the quadratic equation leads to the physical solution:

$$w_{\mathrm{b}} = \frac{1}{2} + \sqrt{\frac{1}{4} - \frac{1}{2} \cdot \frac{N^{same}}{N^D + \overline{N^D} + N^{same}}} \quad (31)$$

The second solution, with the minus sign, always leads to w_{b} values below 0.5.

The probability to correctly identify a quark for the single tag data sample can be used to calculate the probability to correctly identify quark or anti-quark for the double tag data sample:

$$w_{\mathrm{b}}^D = \frac{w_{\mathrm{b}}^2}{w_{\mathrm{b}}^2 + (1 - w_{\mathrm{b}})^2} \quad (32)$$

Hemisphere charge correlations in the events entering the different categories need to be taken into account. For the probability w_{b} for single tagged events these correlations are given by term $\sqrt{1+\delta}$ which is introduced in Equation 31:

$$w_{\mathrm{b}} \cdot \sqrt{1+\delta} = \frac{1}{2} + \sqrt{\frac{1}{4} - \frac{1}{2} \cdot \frac{N^{same}}{N^D + \overline{N^D} + N^{same}}} \quad (33)$$

A similar correlation term, $\sqrt{1+\beta}$, has to be applied for the probability of the double tagged sample, w_{b}^D :

$$w_{\mathrm{b}}^D \cdot \sqrt{1+\beta} = \frac{{w_{\mathrm{b}}}^2 \cdot (1+\delta)}{{w_{\mathrm{b}}}^2 \cdot (1+\delta) + (1 - w_{\mathrm{b}} \cdot \sqrt{1+\delta})^2} \quad (34)$$

A last modification is needed because the selected double tagged data samples contain light and charm quark events in addition to the b quark events. The background events are taken into account by multiplying the different double tagged rates with the corresponding b purities:

$$w_{\mathrm{b}} \cdot \sqrt{1+\delta} = \frac{1}{2} + \sqrt{\frac{1}{4} - \frac{1}{2} \cdot \frac{N^{same} \cdot p_{\mathrm{b}}^{same}}{[N^D + \overline{N^D}\,] \cdot p_{\mathrm{b}}^D + N^{same} \cdot p_{\mathrm{b}}^{same}}} \quad (35)$$

Equation 34 is left unchanged. Equations 35 and 34 are used to extract the flavour tagging probability to measure the b quark forward-backward asymmetry.

References

[1] G.Altarelli et al., *Z PHYSICS AT LEP 1*, CERN 89-08 Volume 1, Geneva 1989.

[2] A.Gurtu, *Precision Tests of the EW Gauge Theory*, summary-talk given at ICHEP2000, Osaka 2000.

[3] The LEP Collaborations, *A Combination of Preliminary Electroweak Measurements and Constraints on the Standard Model*, CERN-EP in preparation.

[4] DELPHI Collaboration, P. Abreu et al., Eur. Phys. J. **C9** (1999) 367.

[5] DELPHI Collaboration, P. Antilogous et al., contributed paper 377 to ICHEP2000, Osaka 2000.

[6] DELPHI Collaboration, P.Abreu et al., Nucl. Instr. Meth. **A303** (1991) 233;
DELPHI Collaboration, P.Abreu et al., Nucl. Instr. Meth. **A378** (1996) 57.

[7] T. Sjostrand, P. Eden, C. Friberg, L. Lonnblad, G. Miu, S. Mrenna and E. Norrbin, hep-ph/0010017.

[8] DELPHI Collaboration,P. Abreu et al. Z. Phys. **C73** (1996) 11.

[9] ALEPH Collaboration, D.Buskulic et al., Phys. Lett. **B313** (1993) 535.

[10] G.Borisov, C.Mariotti, Nucl. Instr. Meth. **A372** (1996) 181.

[11] DELPHI Collaboration, P.Abreu et al., E. Phys. J. **C10** (1999) 415.

[12] The Particle Data Group, D.E.Groom et al., Euro. Phys. J. **C15** (2000) 1.

[13] T. Allmendinger, G. Barker, M. Feindt, C. Haag, M. Moch, hep-ex/0102001.

[14] D.Bardin et al., *ZFITTER: An Analytical Program for Fermion Pair Production in e^+e^- Annihilation*, CERN-TH 6443, Geneva 1992.

[15] D.Abbaneo et al., *QCD corrections to the forward-backward asymmetries of c and b quarks at the Z pole*, Eur. Phys. J. **C4** (1998) 185.

[16] The LEP Collaborations, *A Combination of Preliminary Electroweak Measurements and Constraints on the Standard Model*, CERN-EP/2000-016, Genf 2000.

[17] OPAL Collaboration, G.Abbiendi et al., E. Phys. J. **C13** (2000) 1.

[18] The LEP Heavy Flavour Group, *Input Parameters for the LEP/SLD Electroweak Heavy Flavour Results for Summer 1998 Conferences*, LEPHF/98-01.

[19] The LEP Collaborations, *A Combination of Preliminary Electroweak Measurements and Constraints on the Standard Model*, CERN-EP/99-15, Genf 1999;
The LEP Collaborations, Nucl. Inst. Meth. **A378** (1996) 101.

[20] MARK III Collaboation, D. Coffman et al., Phys. Lett. **B263** (1991) 135.

[21] ALEPH, CDF, DELPHI, L3, OPAL and SLD Collaborations, D.Abbaneo et al., *Combined results on b-hadron production rates, lifetimes, oscillations and semileptonic decays*, hep-ex/0009052.

[22] ALEPH Collaboration, R.Barate et al., Phys. Lett. **B426** (1998) 217.

[23] L3 Collaboration, M.Acciarri et al., Phys. Lett. **B439** (1998) 225.

[24] OPAL Collaboration, K.Ackerstaff et al., Z. Phys. **C75** (1997) 385.

[25] ALEPH Collaboration, D.Buskulic et al., Phys. Lett. **B384** (1996) 414.

[26] DELPHI Collaboration, P.Abreu et al., Z. Phys. **C65** (1995) 569.

[27] L3 Collaboration, O.Adriani et al., Phys. Lett. **B292** (1992) 454.

[28] OPAL Collaboration, G.Alexander et al., Z. Phys. **C70** (1996) 357.

[29] SLD Collaboration, K. Abe et al. Phys. Rev. Lett. **84** (2000) 5945, hep-ex/0004026.